IN-18
14427
869

NASA Technical Memorandum 4289

Atmospheric Turbulence Review of Space Shuttle Launches

Michael Susko

MAY 1991

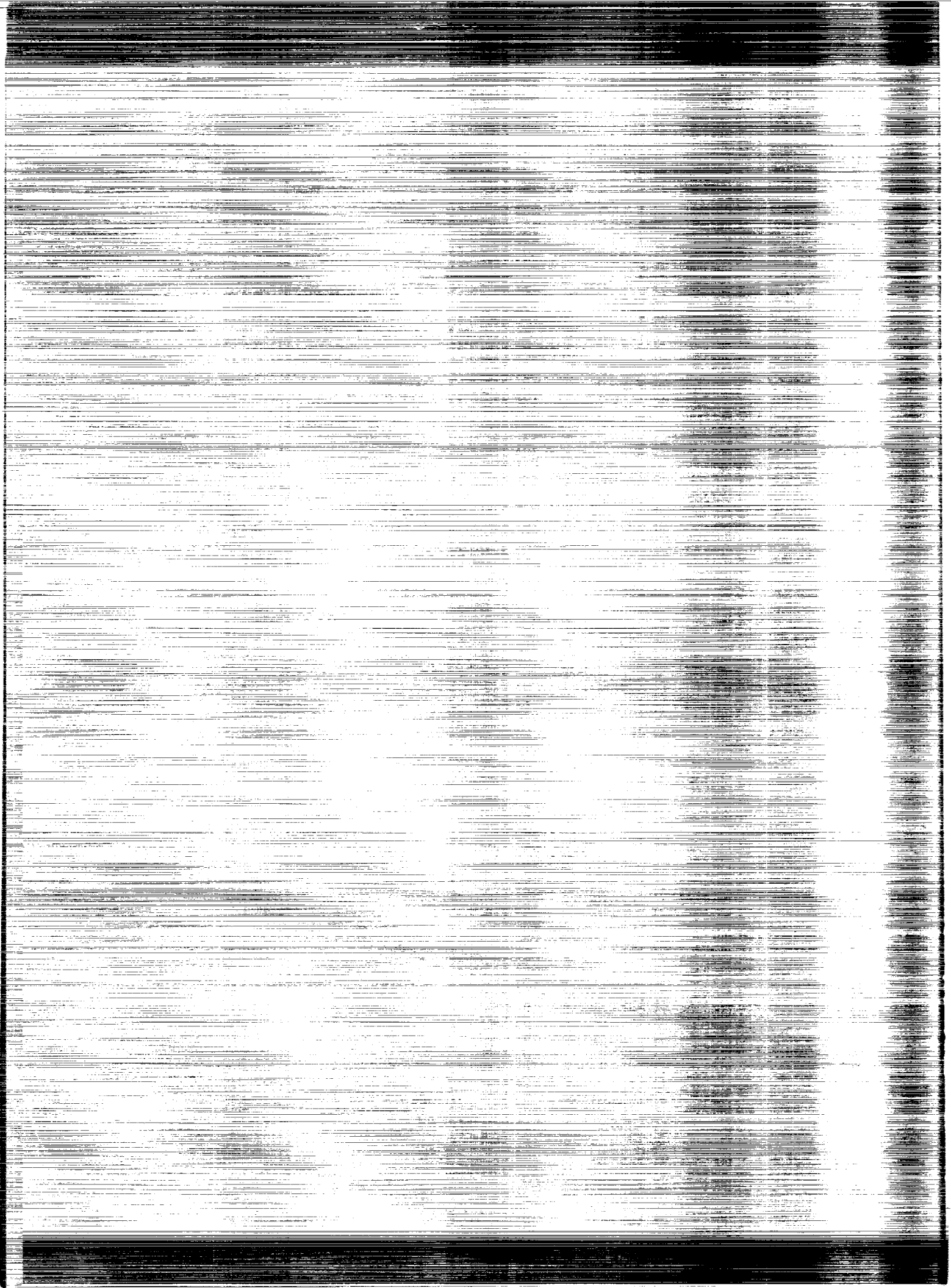

NASA Technical Memorandum 4289

Atmospheric Turbulence Review of Space Shuttle Launches

Michael Susko
George C. Marshall Space Flight Center
Marshall Space Flight Center, Alabama

National Aeronautics and
Space Administration
Office of Management
Scientific and Technical
Information Division

1991

ACKNOWLEDGMENTS

The help of Glen W. Batts, Sr., staff analyst, New Technology, Inc., Huntsville, Alabama, is gratefully acknowledged.

TABLE OF CONTENTS

LIST OF ILLUSTRATIONS

LIST OF ILLUSTRATIONS (Continued)

LIST OF ILLUSTRATIONS (Continued)

LIST OF ILLUSTRATIONS (Continued)

TECHNICAL MEMORANDUM

ATMOSPHERIC TURBULENCE REVIEW OF SPACE SHUTTLE LAUNCHES

I. INTRODUCTION

The main purpose of this paper is to report on the research and analysis on identifying turbulent regions from the surface to 16 km for the space shuttle launches. It will be demonstrated that the FPS-16 radar/jimsphere balloon system, in conjunction with the rawinsonde, can indicate the presence of turbulence or that the conditions are ripe for turbulence during the day-of-launch scenario.

The existing technology for the past three decades (60's, 70's, and 80's) in measuring winds aloft for the space shuttle launches has been obtained by balloon-borne wind sensors, e.g., the FPS-16 radar/jimsphere system (used as the standard) and the meteorological sounding system (MSS) windsonde (used as the backup) and was documented by Susko [1]. The wind profiles are measured in the lower stratosphere and troposphere of the atmosphere (0 to 16 km) for the wind load analysis of the ascent phase of the space shuttle as it passes through max q (maximum dynamic pressure) where the loads are the greatest on the vehicle.

Further use of the jimsphere can be expanded to obtain turbulence data for the space shuttle launches. The atmospheric data obtained during the shuttle launches by the rawinsonde provide the necessary meteorological data to compute aerodynamic parameters to identify turbulence. The aerodynamic parameters calculated from the measurements indicate the presence of turbulence or conditions ripe for turbulence were the Reynolds number, drag coefficient, turbulent stresses, total energy, stability parameter, vertical gradient of kinetic energy, Richardson number, and the turbulence probability index. However, even though the indicators may be showing the presence of turbulence, an in situ sensor, or pilot experiencing turbulence while the balloon is in the air, would eliminate the uncertainty that the atmosphere is actually turbulent.

II. DYNAMICS OF TURBULENCE—SPACE SHUTTLE

One meteorological feature used in describing the dynamics of turbulence is to delineate between turbulence and no turbulence which is the vertical gradient of kinetic energy as reported by Ehernberger [2]. The value of this gradient has been derived as the product of wind speed and vertical wind shear measurements obtained directly from jimsphere data. This parameter has been analyzed during the six space shuttle flights where the vertical gradient of kinetic energy was computed

$$KE = V(dV/dH) \quad . \tag{1}$$

The kinetic energy gradient plots which illustrate very good results between turbulence (*T*) and no turbulence (*NT*) during shuttle launches are given in appendix A, figures 1g(*T*), 2g(*T*), 3g(*NT*), 4g(*T*), 5g(*NT*), and 6g(*NT*).

The dynamics and time scales of regions of active turbulence are fairly complicated. It is generally conceded that the turbulence is initiated by Kelvin-Helmholtz instability when the Richardson number decreases to a value near 0.25. Several physical processes can cause this decrease. Nonturbulent portions of the atmosphere are subjected to fluctuations in shear and/or potential temperature gradient caused by gravity wave disturbances. These fluctuations may cause turbulence. Synoptic and mesoscale dynamical processes also cause evolutions in the shear and lapse rates which can cause turbulence.

Once a layer of thickness, *Z*, becomes turbulent, it is of interest to ponder the temporal duration of the turbulent event. If the turbulence is caused by a gravity wave fluctuation, then Fairall et al. [3] indicates that the event will last not more than a fraction of an inertial period (say, a few hours). If the breakdown is due to synoptic processes, then in principle the turbulence can endure as long as the Richardson number can maintain the instability against turbulent mixing.

From the rawinsonde data obtained from the meteorological section, Cape Canaveral Air Force Station, Florida, which consists of winds, temperature, and pressure as a function of altitude and the winds from the jimsphere, the Richardson number, a stability criteria for determining the presence or absence of atmospheric turbulence, was computed and is given by the following relationship:

$$R_i = \frac{g}{T}\left[\frac{\partial T}{\partial Z} + \Gamma\right] \Big/ \left[\frac{\partial V}{\partial Z}\right]^2 \tag{2}$$

where g is the acceleration of gravity $\partial T/\partial Z$ is the vertical temperature gradient, Γ is the dry adiabatic lapse rate, 9.8 C/km, and

$$\left[\frac{\partial V}{\partial Z}\right]^2 = \left[\frac{\partial V_x}{\partial Z}\right]^2 + \left[\frac{\partial V_y}{\partial Z}\right]^2$$

is the square of the vertical shear of the horizontal winds.

The Richardson number plots for the six space shuttle launches, figures 1h(*T*), 2h(*T*), 3h(*NT*), 4h(*T*), 5h(*NT*), and 6h(*NT*), are given in appendix A. Since instabilities of turbulence increase when the Richardson number decreases to a value near 0.25, the Richardson number was inverted for clarity, indicating turbulence with the larger numbers.

2.1 Tropopause

The tropopause is an ideal boundary for the generation of large-scale turbulence due to the change with elevation from an adiabatic lapse rate to one of nearly constant temperature as reported by Otten and Rose [4].

Tropopause height is defined as the altitude where the inflection point occurs in the ambient temperature when plotted as a function of mean sea level. The dramatic increase of the atmospheric structure constant of temperature is a behavior to assess in turbulence.

An idealized tropopause is envisioned that is an annular region concentric to the Earth's surface. In reality, the tropopause is convoluted by synoptic meteorology and varies in altitude due to changes in season and latitude.

The principle for clear air turbulence (CAT) is that CAT is found statistically more often within inversion layers and at the tropopause. The term "inversion layer" refers to a layer within which temperature, centigrade or Kelvin, increases with an increasing altitude.

Appendix A, figures 1e(*T*), 2e(*T*), 3e(*NT*), 4e(*T*), 5e(*NT*), and 6e(*NT*), gives the wind speed, wind direction, and temperature plots. Note the atmospheric inversion layer at the tropopause, figures 1e, 2e, and 4e.

2.2 Stratosphere

In his laboratory studies, Murtele [5] used the best data to show the situation of the famous United Airlines episode which occurred in the stratosphere over Hannibal in 1981 where there was quite a bit of damage and injury inside the plane. The author concluded that the only thing necessary for a highly reflective and potentially turbulent situation is a reasonably deep layer of decreasing wind speed. (By decreasing, the author means it is lower at higher levels than at lower levels.) This is fairly characteristic of the stratosphere. So it suggests that the structure of the lowest stratosphere is often extremely important as far as clear-air turbulence is concerned. In his studies, flow that reversed itself from between 25 and 30 m/s to -25 m/s should show violent vertical updrafts, and a very turbulent region would result. This is very similar to jimsphere data where the rise rate of the balloon would increase from 5 m/s to 8 or 9 m/s, indicating a turbulent region.

Turbulence is a state of flow "in which the instantaneous velocities exhibit irregular and apparently random fluctuations so that in practice only statistical properties can be recognized and subjected to analysis. These fluctuations often constitute major deformations of the flow, and are capable of transporting momentum energy and suspended matter at rates far in excess of the rate of transport by the molecular processes of diffusion and conduction in nonturbulent or laminar flow," Huschke [6].

The wind variation depends on the sensitivity of instrumentation, time of measurement, and averaging. All of these factors affect the wind shear. Factors affecting the vertical motion of a zero-pressure polyethylene, free balloon were explored by Dwyer [7]. Because the balloon has no single characteristic length, a third dimensionless variable, fractional volume is needed. Its inconsistent shape and shape deformation further complicate the computation of Reynolds number, drag coefficient, and Froude number. The jimsphere, however, is a constant 2-m diameter balloon, as indicated by Scoggins [8].

The basis of the proposed numerical forecasting of buffeting and the resulting turbulence of aircraft is observed under those conditions where the vertical gradient of air temperature, wind direction, and speed exceed the critical values. The details of forecasting are reported by Perevedentsev [9]. The following values were established as the critical values of vertical gradients for air temperature (7 °C per km of altitude), for wind velocity (10 m/s per km of altitude), and for wind direction (15° per km of altitude). The buffeting of airplanes is indicated in the layer in which one of the listed vertical gradients is higher than critical. At those altitudes where two conditions for increased turbulence are satisfied simultaneously, the greatest probability and intensity of buffeting are expected.

III. DISCUSSION—FPS-16 RADAR/JIMSPHERE BALLOON SYSTEM

Vertical wind motions in the atmosphere are very easily detected by the FPS-16 radar/jimsphere system, as described by Endlich et al. [10], Fichtl et al. [11], DeMandel and Krivo [12], Kaufman and Susko [13], Johnson and Vaughan [14], and Hill [15]. By means of low-pass filtering, high-frequency noise introduced by the FPS-16 radar is eliminated from the vertical rise rate jimsphere data. The remaining perturbations may be representative of the induced vertical motions. Normally, the jimsphere rises about 5 m/s from sea level to 16 km as described by Scoggins [16], MacCready and Jex [17], Vaughan [18], Susko and Kaufman [19], Johnson and Vaughan [14], and Hill [15]. MacCready and Jex [17] stated that the value of the drag coefficient is of primary importance in computing the response of a jimsphere or any other balloon to a change in wind speed. This was confirmed by Scoggins [8] in his article "Aerodynamics of Spherical Balloon Wind Sensor." Kaufman and Susko [13] indicated that the drag coefficient is small at supercritical Reynolds number (Re) where the turbulent wake is small, but increases sharply in the transition region. The C_D is higher in subcritical Re where the wake is larger and the flow is laminar.

Jimsphere vertical rise rate data have been observed to vary from 2 to 10 m/s. Figure 1 illustrates some C_D versus Re values calculated for various vertical rise rates from the U.S. Standard Atmosphere (1962) temperature profile data. Figure 2 shows the following jimsphere vertical rise rate data: profile A was observed from the jimsphere, released at 1525Z, March 4, 1969, at Wallops Island, and profile B was observed from the jimsphere released at 1933Z, March 5, 1969, also at Wallops Island. Profile A shows a typical 5-m/s rise rate from 10 to 12 km layer; whereas, profile B shows the rise rate to be about 7 m/s. The corresponding C_D versus Re values from profiles A and B are plotted in figure 1, where the lower C_D at higher Re suggests a smaller turbulent wake downstream from the jimsphere. This in turn suggests a layer of significant turbulence compared to turbulence of the adjacent air layers. Figure 3 shows the scalar wind-speed profiles A and B. Notice the jet stream wind speed of approximately 100 m/s between 10 and 12 km of profile B which relates to the resultant variation (turbulence) in the C_D versus Re values in figure 1.

Appendix A gives the jimsphere rise rate versus altitude, figures 1a(T), 2a(T), 3a(NT), 4a(T), 5a(NT), and 6a(NT); and the Re and C_D versus altitude, figures 1c(T), 2c(T), 3c(NT), 4c(T), 5c(NT), and 6c(NT), for the six space shuttle launches.

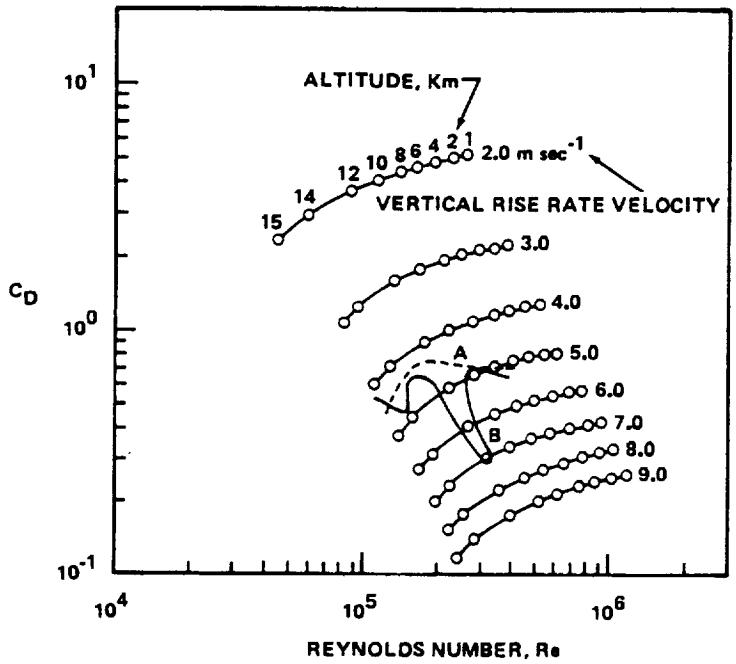

Figure 1. Idealized C_D versus Re curves as calculated from standard atmospheric data, and results calculated from jimsphere release A, March 4, 1969 (1525Z) and release B, March 6, 1969 (1933Z).

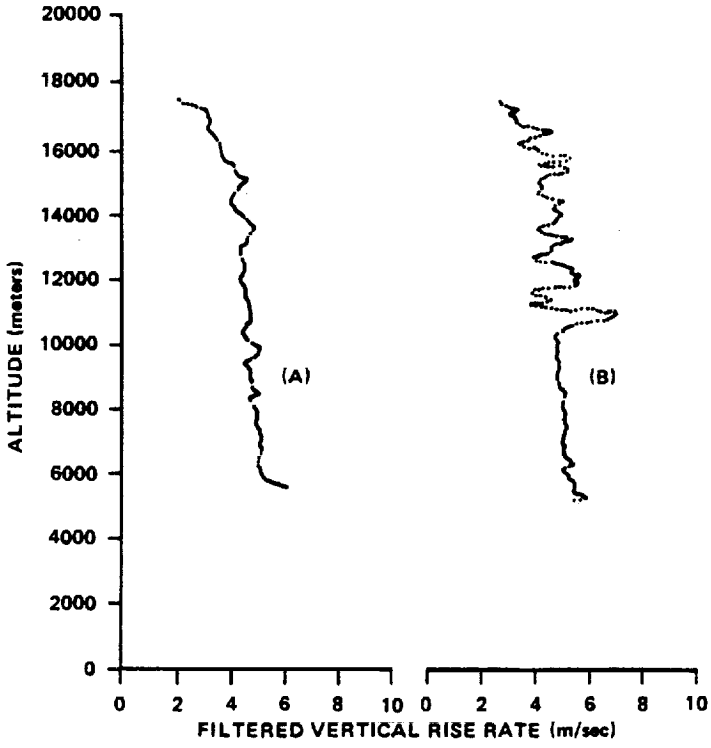

Figure 2. Vertical rise rate of jimsphere releases at Wallops Station, Virginia. Jimsphere A was released on March 4, 1969 (1525Z). Jimsphere B was released on March 6, 1969 (1933Z).

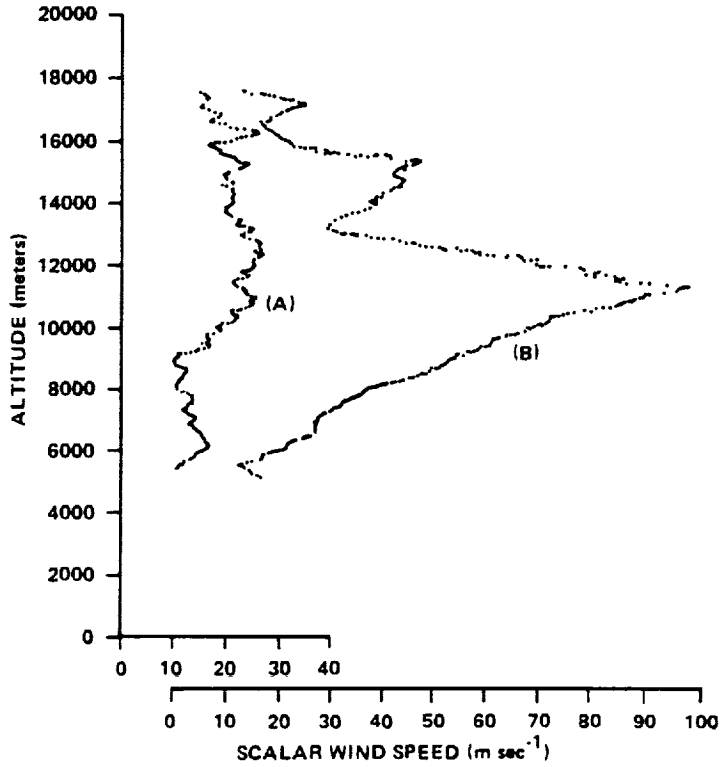

Figure 3. Vertical wind profiles measured by the FPS-16 radar/jimsphere at Wallops Island, Virginia. Jimsphere A was released on March 4, 1969 (1525Z). Jimsphere B was released on March 6, 1969 (1933Z). The wind variation depends on the sensitivity of instrumentation.

3.1 Jimsphere Balloon Data Assessment

Data from the jimsphere balloon are calculated every 30 m and averaged over a scale length of 150 m in altitude. The length scale was made at 150-m intervals because the discernible wavelengths of the jimsphere are on the order of 100 to 150 m, as noted by Endlich et al. [10], Susko [20], and Smith [21].

Measurements of the meteorological parameters were made by the jimsphere and rawinsonde. Aerodynamic parameters calculated from the measurements to identify turbulence were the Reynolds number, drag coefficient, turbulent stresses, total energy, stability parameter, kinetic energy, Richardson number, and the turbulence probability index. These measurements were computed from 16 jimsphere balloon releases obtained during space shuttle launched at KSC. For simplicity and clarity, six of the launches illustrating examples of no turbulence and turbulence in the atmosphere are presented in this report.

3.1.1 Reynolds Number and Drag Coefficient

The Reynolds number is a nondimensional ratio of the inertial force to the viscous force in fluid motion ·

$$Re' = \frac{L\,U}{\gamma} \quad , \tag{3}$$

where L is a characteristic length, U is a characteristic velocity, and γ is the kinematic viscosity. The Reynolds number (Re) is an index of performance, and in the theory of hydrodynamic stability, it is the origin of turbulence. Assuming an incompressible adiabatic, steady flow of a homogeneous fluid, then the only force is the impact or inertial force to the viscous force.

In the calculation of the aerodynamic parameters in this paper, L (the characteristic length) is 2 m, the diameter of the jimsphere balloon and U (the characteristic velocity) is the rise rate of the jimsphere balloon.

Appendix A, figures 1b,c(T); 2b,c(T); 3b,c(NT); 4b,c(T); 5b,c(NT); and 6b,c(NT) gives the plots of Re versus C_D and Re versus altitude, illustrating the behavior of the jimsphere in the atmosphere.

The drag coefficient (C_D) is a dimensionless ratio of (a) the component of a force parallel to the direction of flow (drag) excited on a body by a fluid in the kinetic energy of the fluid by a characteristic surface area of the body. In symbols, the drag coefficient C_D is as follows:

$$C_D = \frac{F_B}{1/2\ \rho V^2 s} \quad , \tag{4}$$

where F_B is the force of resistance (buoyant force), ρ is fluid density, V is the wind speed, and s is the surface area of the jimsphere balloon. Additional details are reported in reference 22.

Appendix A, figures 1b,c(T); 2b,c(T); 3b,c(NT); 4b,c(T); 5b,c(NT); and 6b,c(NT), illustrates the behavior of C_D with altitude for the jimsphere balloon.

3.1.2 Turbulent Stresses

The turbulent stresses are the representation of the transfer of momentum due to turbulent fluctuations. The turbulent stress is given by the equation;

$$U_*^2 \equiv \sqrt{\overline{u'w'}^2 + \overline{v'w'}^2} \quad , \tag{5}$$

which is the square root of the time average (the bar indicates a time average) of the square of the eddy velocities of u' and w' and v' and w'.

Appendix A, figures 1f(T), 2f(T), 3f(NT), 4f(T), 5f(NT), and 6f(T), illustrates the behavior of the turbulent stresses versus altitude during the six space shuttle launches.

3.1.3 Total Energy

The total energy (e) obtained by the jimsphere balloon wind measurement was calculated from the equation

$$e \equiv \frac{1}{2} (\overline{u}'^2 + \overline{v}'^2 + \overline{w}'^2) \ . \tag{6}$$

The total energy is the time average of the square of the eddy velocities of u', v', and w' in m^2/s^2.

Appendix A, figures 1f(T), 2f(T), 3f(NT), 4f(T), 5f(NT), and 6f(NT), illustrates the fluctuations of e with altitude for the six space shuttle launches.

3.1.4 Stability Parameter

The stability parameter (ξ), obtained from the jimsphere balloon wind measurements and the temperature from the radiosonde, was calculated from the equation $\xi = X/L$ where

$$L = -\frac{\overline{T}\, U_*^3}{kg\ \overline{w'T'}} \ , \tag{7}$$

T is the temperature in degrees K, U_* is the stress from equation (5), k is Von Karman's constant, w' is the vertical velocity perturbation, g is the acceleration of gravity, and X is the scale height as reported in reference 23.

Appendix A, figures 1f(T), 2f(T), 3f(NT), 4f(T), 5f(NT), and 6f(NT), illustrates the stability parameter versus altitude for the six space shuttle launches.

3.1.5 Turbulence Probability Index

Turbulence probability index (T_I) was reported by Endlich [10], and further defined in reference 24 where $T_I = A\ B$.

Factor A, which is the wind directional shear, is given by the equation

$$A = S|\Delta\alpha/\Delta z| \ , \tag{8}$$

where S is wind speed and $\Delta\alpha$ is the change in wind direction over the scale length of Δz.

The second factor B is equal to the change in temperature lapse rate. The equation is

$$B = [(g/T)|\Delta^2 T/\Delta z|]^{1/2} , \tag{9}$$

where g is the acceleration of gravity and $\Delta^2 T$ is the second difference operator of the temperature T. The two factors are multiplied together, resulting in $T_I = AB$.

Appendix A, figures 1d(T), 2d(T), 3d(NT), 4d(T), 5d(NT), and 6d(NT), illustrates T_I versus altitude for the six space shuttle launches for turbulence and no turbulence.

IV. SUMMARY

This research has demonstrated that the results of measurements of winds aloft from the FPS-16 radar/jimsphere balloon system can indeed indicate the presence or conditions ripe for turbulence in the troposphere and lower stratosphere (0 to 16 km). It has been shown with wind measurement data obtained during six space shuttle launches by the jimsphere balloon, in conjunction with the rawinsonde which provides temperature and pressure data as a function of altitude that the aerodynamic parameters calculated can indicate the presence of turbulence. There is no magic fool-proof criteria in atmospheric turbulence probability of occurrence. However, the occurrence of turbulence at the tropopause is identified by the enhanced temperature lapse rates and enhanced inversion rates, strong vector wind shears, and large changes in wind direction. When any two of the above conditions occur simultaneously, a significant probability of turbulence can occur as shown in this report. However, even though the indicators may be showing the presence of turbulence, an in situ sensor or pilot experiencing turbulence while the balloon is in the air would eliminate the uncertainty that the atmosphere is actually turbulent.

APPENDIX A

Figures 1 through 6 (where figures 1, 2, and 4 illustrate turbulence (*T*), and figures 3, 5, and 6 show essentially no turbulence (*NT*)).

a. Balloon rise rate versus altitude.

b. Reynolds number versus drag coefficient.

c. Reynolds number and drag coefficient versus altitude.

d. Turbulence probability indicator versus altitude.

e. Wind speed, wind direction, and temperature versus altitude.

f. Total energy, stress, stability parameter versus altitude.

g. Kinetic energy versus altitude.

h. Richardson number versus altitude.

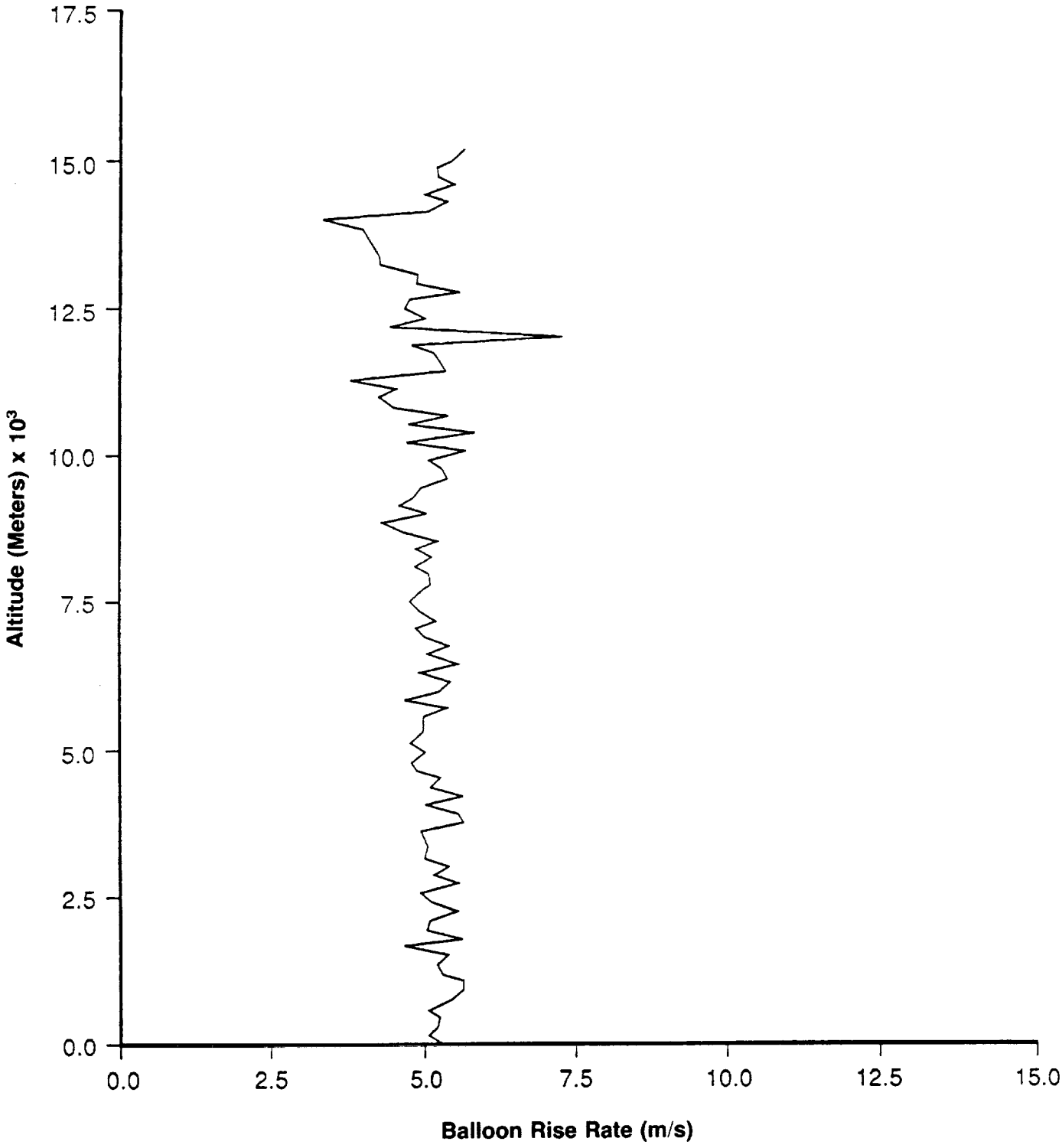

Figure 1a. Rise rate of FPS-16 radar/jimsphere balloon ascent obtained during STS-11 launch, February 3, 1984 (1300Z) at KSC, Florida.

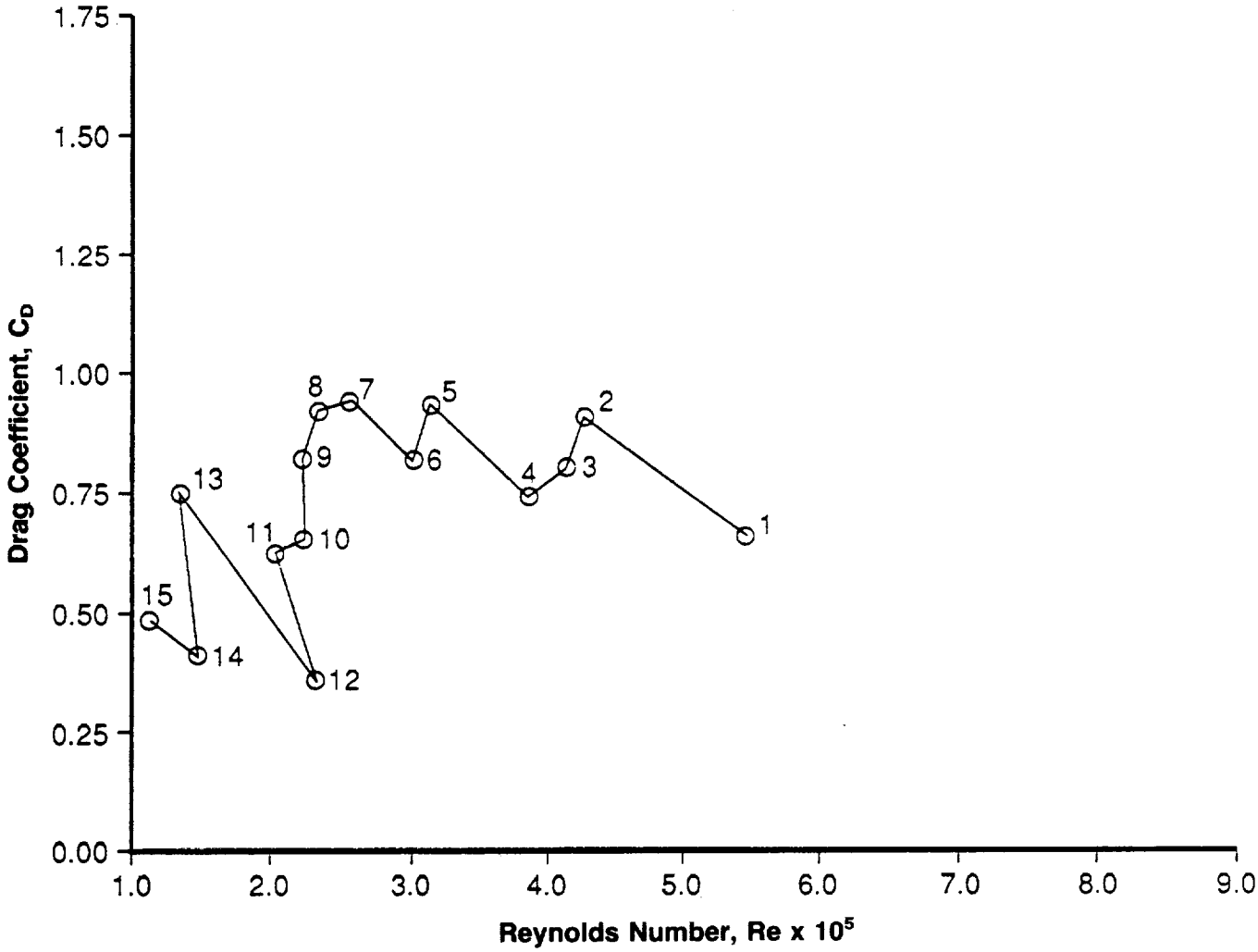

Figure 1b. C_D versus *Re* parameter obtained from FPS-16 radar/jimsphere balloon ascent during STS-11 launch, February 3, 1984 (1300Z) at KSC, Florida.

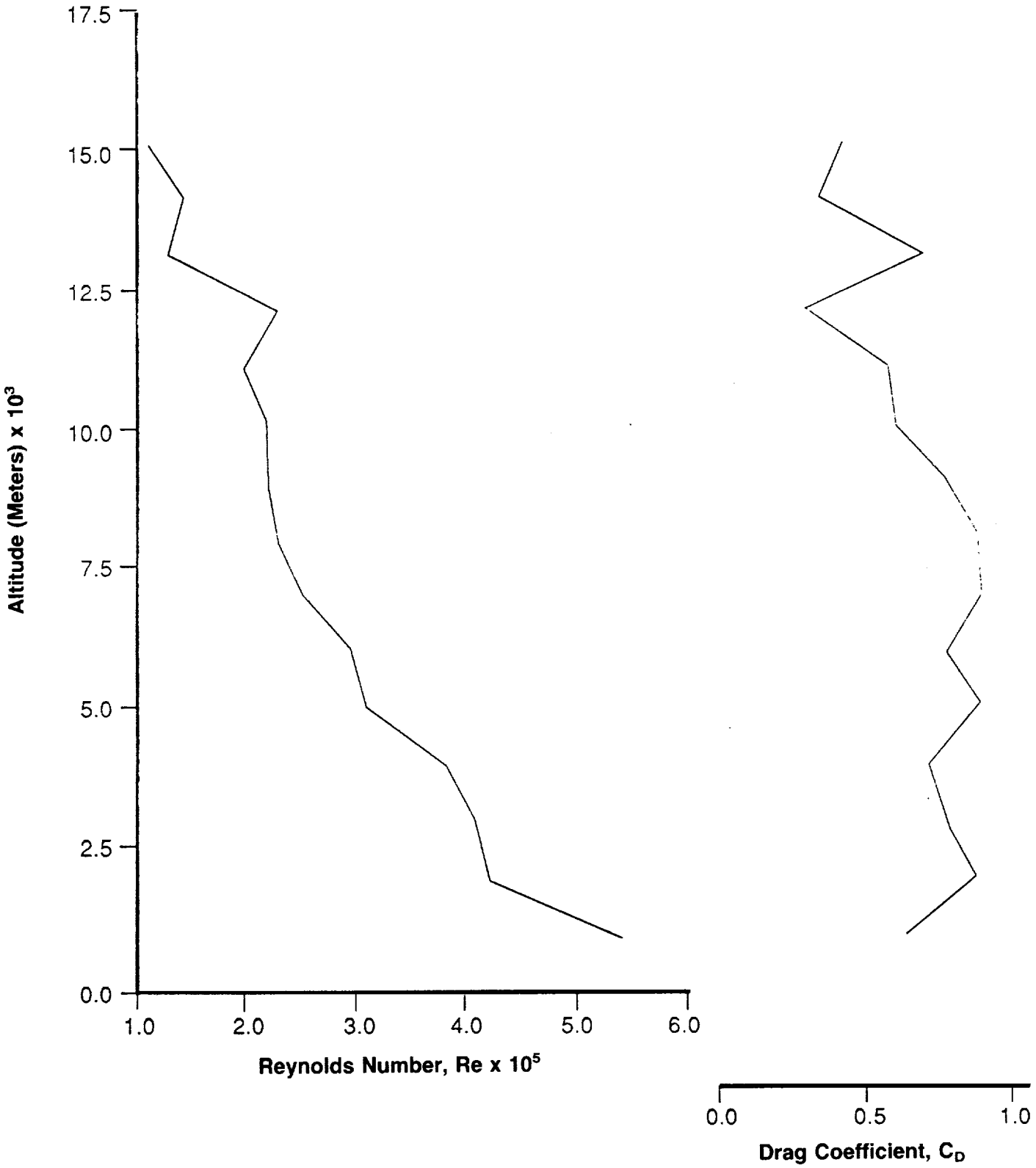

Figure 1c. C_D and *Re* altitude plots obtained from FPS-16 radar/jimsphere balloon ascent during STS-11 launch, February 3, 1984 (1300Z) at KSC, Florida.

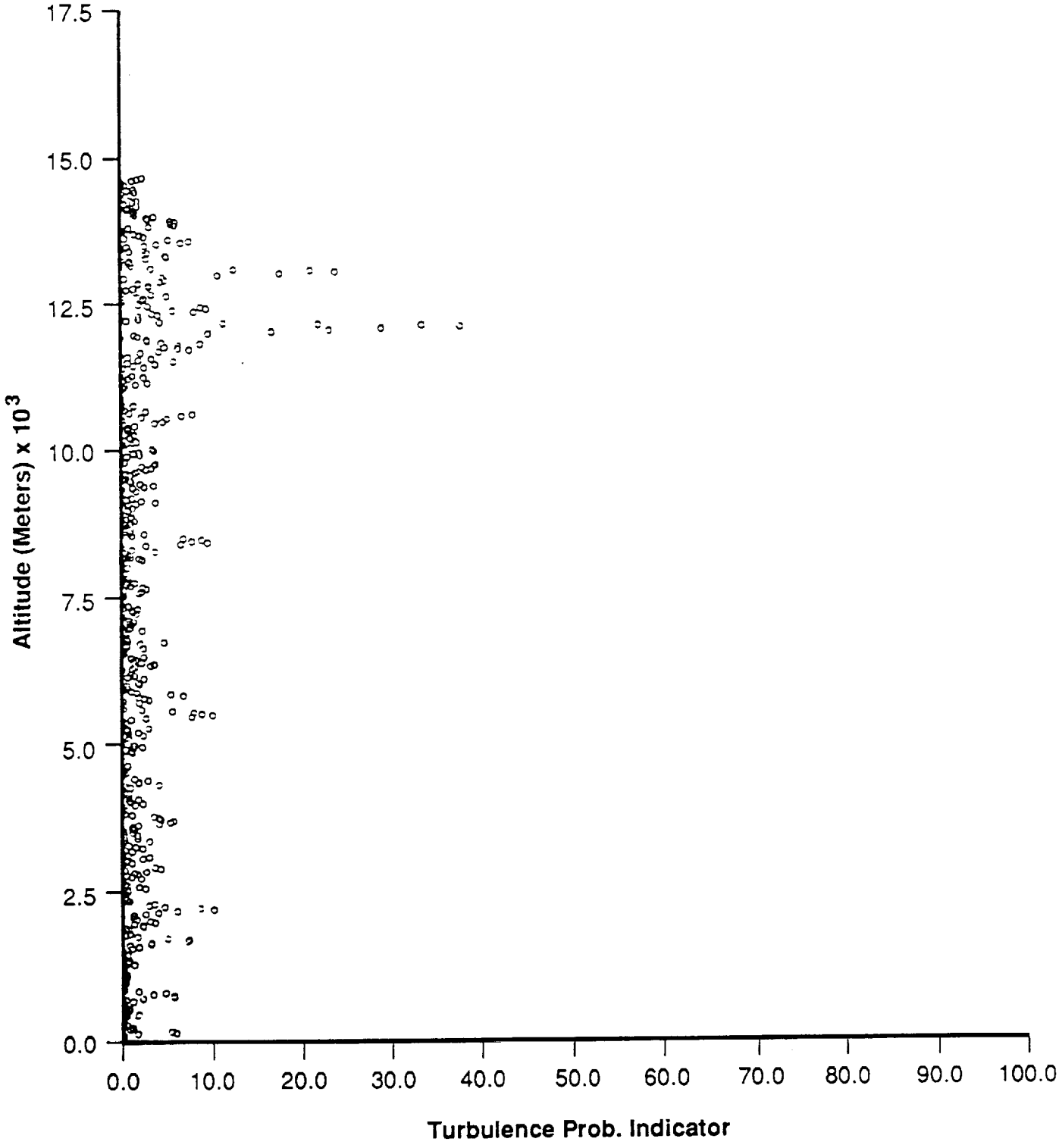

Figure 1d. Turbulence probability indicator obtained during STS-11 launch, February 3, 1984 (1300Z) at KSC, Florida.

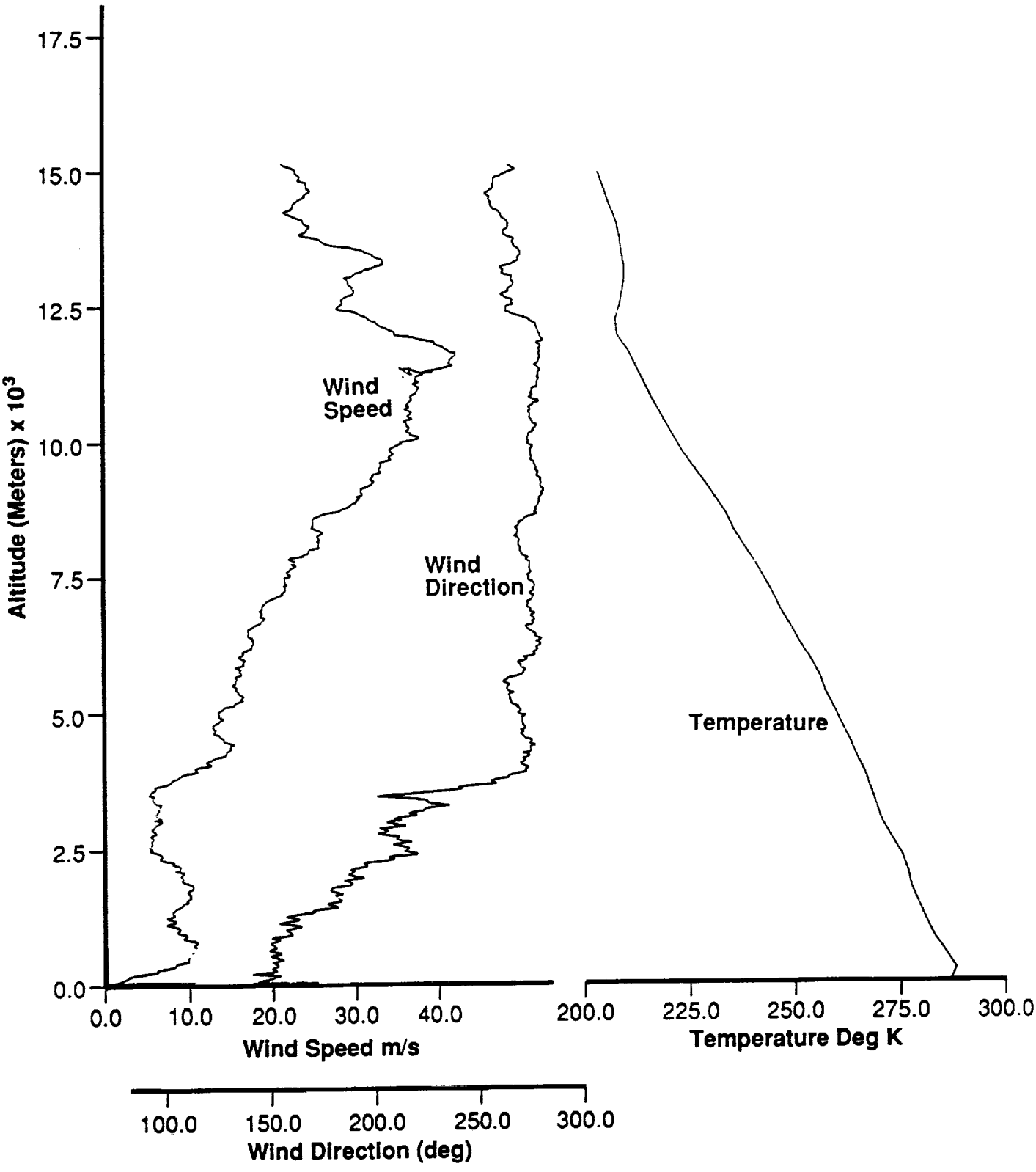

Figure 1e.. Wind speed, wind direction, and temperature versus altitude plots measured during STS-11 launch, February 3, 1984 (1300Z) at KSC, Florida.

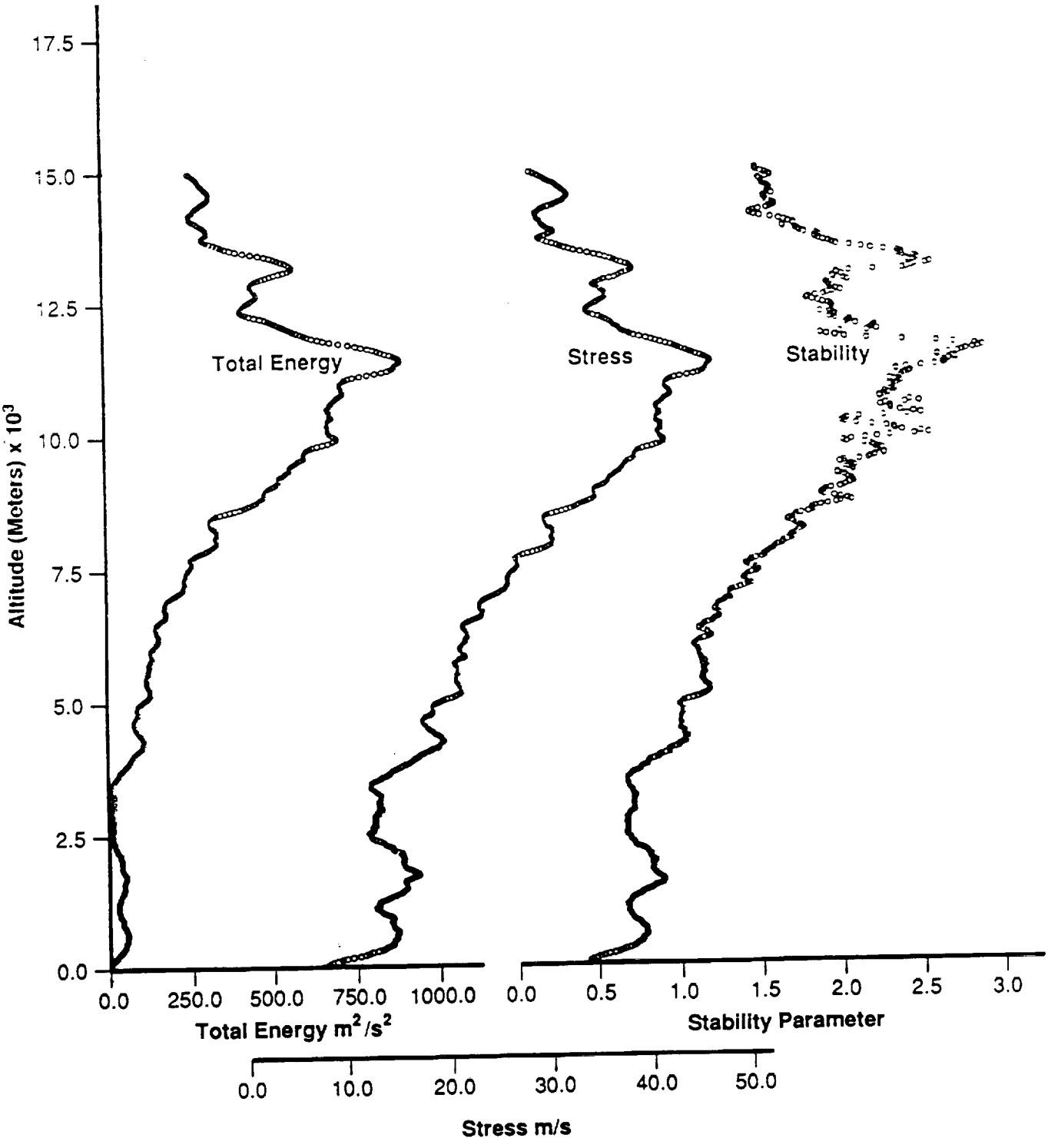

Figure 1f. Total energy, stress, and stability versus altitude parameters during STS-11 launch, February 3, 1984 (1300Z) at KSC, Florida.

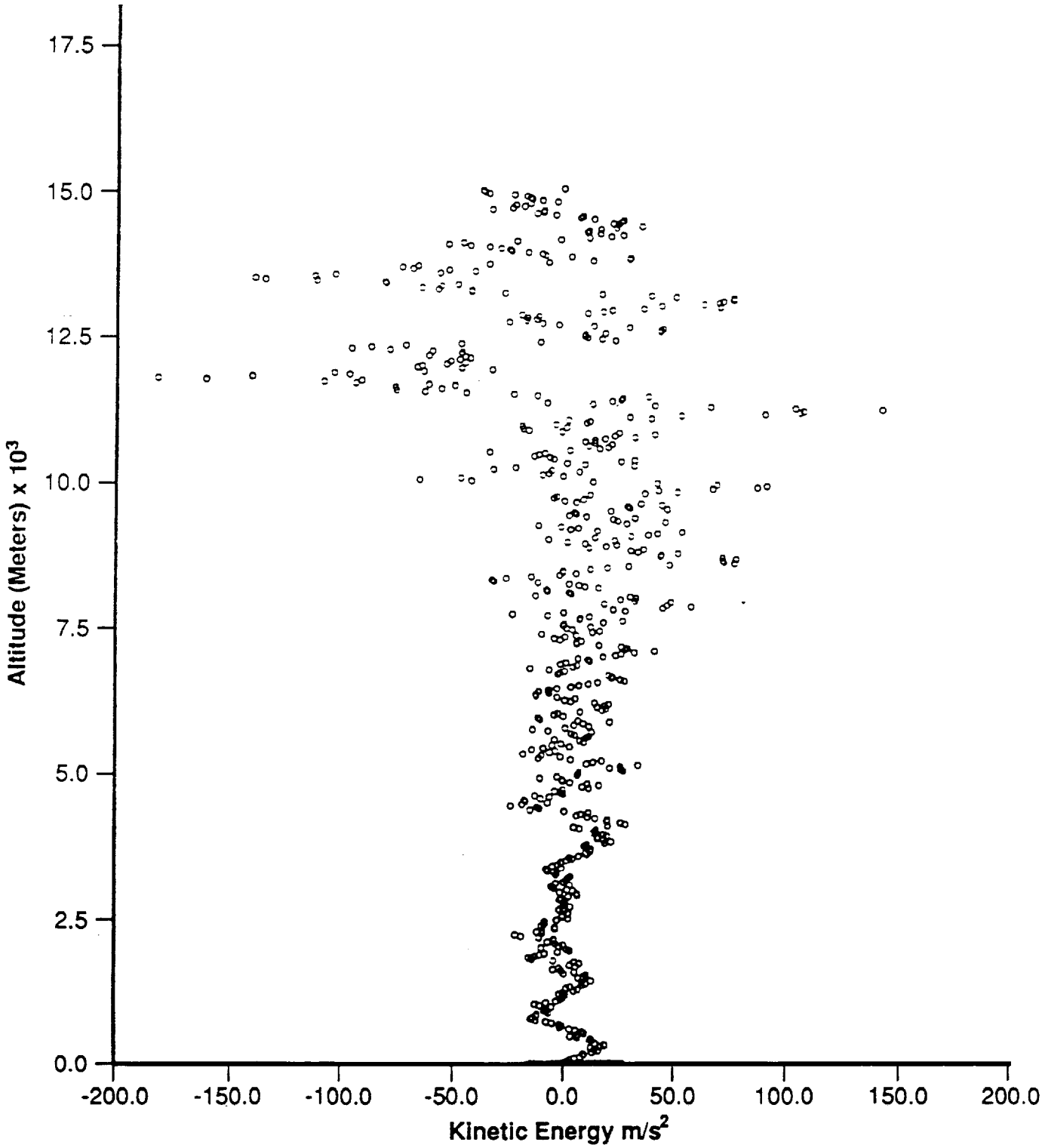

Figure 1g. Kinetic energy versus altitude parameter for STS-11 launch, February 3, 1984 (1300Z) at KSC, Florida.

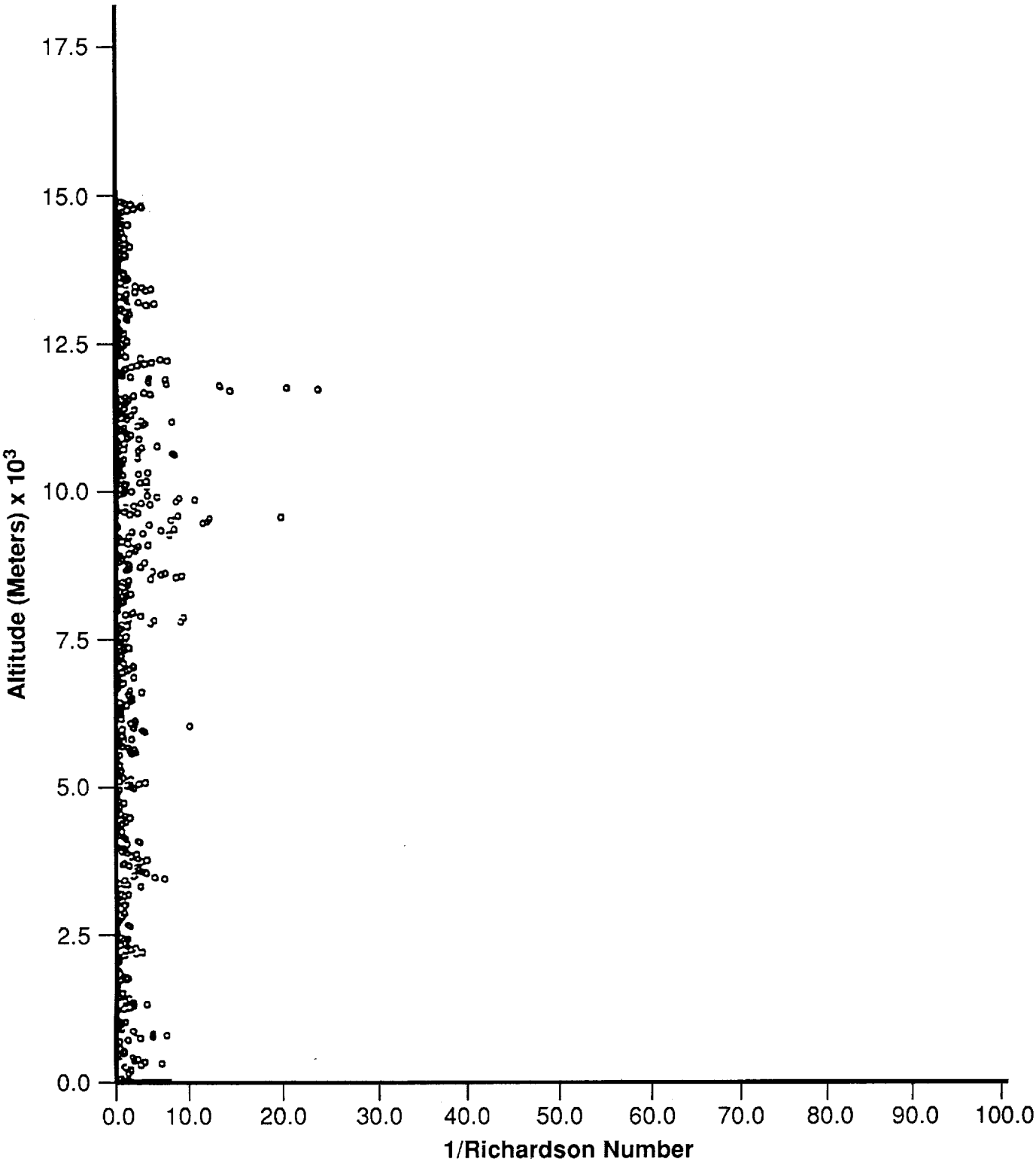

Figure 1h. Richardson number versus altitude parameter for STS-11 launch, February 3, 1984 (1300Z) at KSC, Florida.

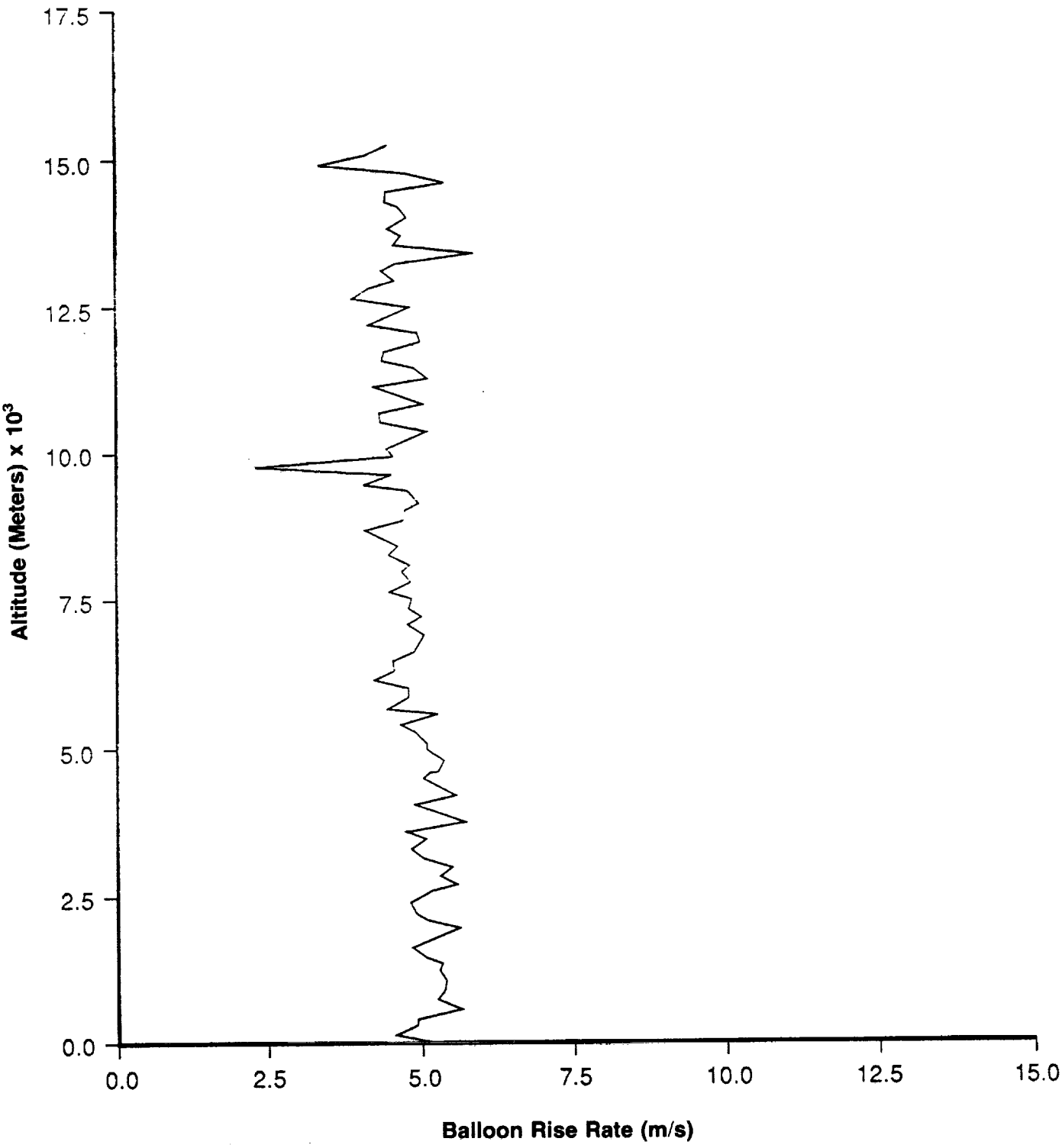

Figure 2a. Rise rate of FPS-16 radar/jimsphere balloon ascent obtained during STS-13 launch, April 6, 1984 (1358Z) at KSC, Florida.

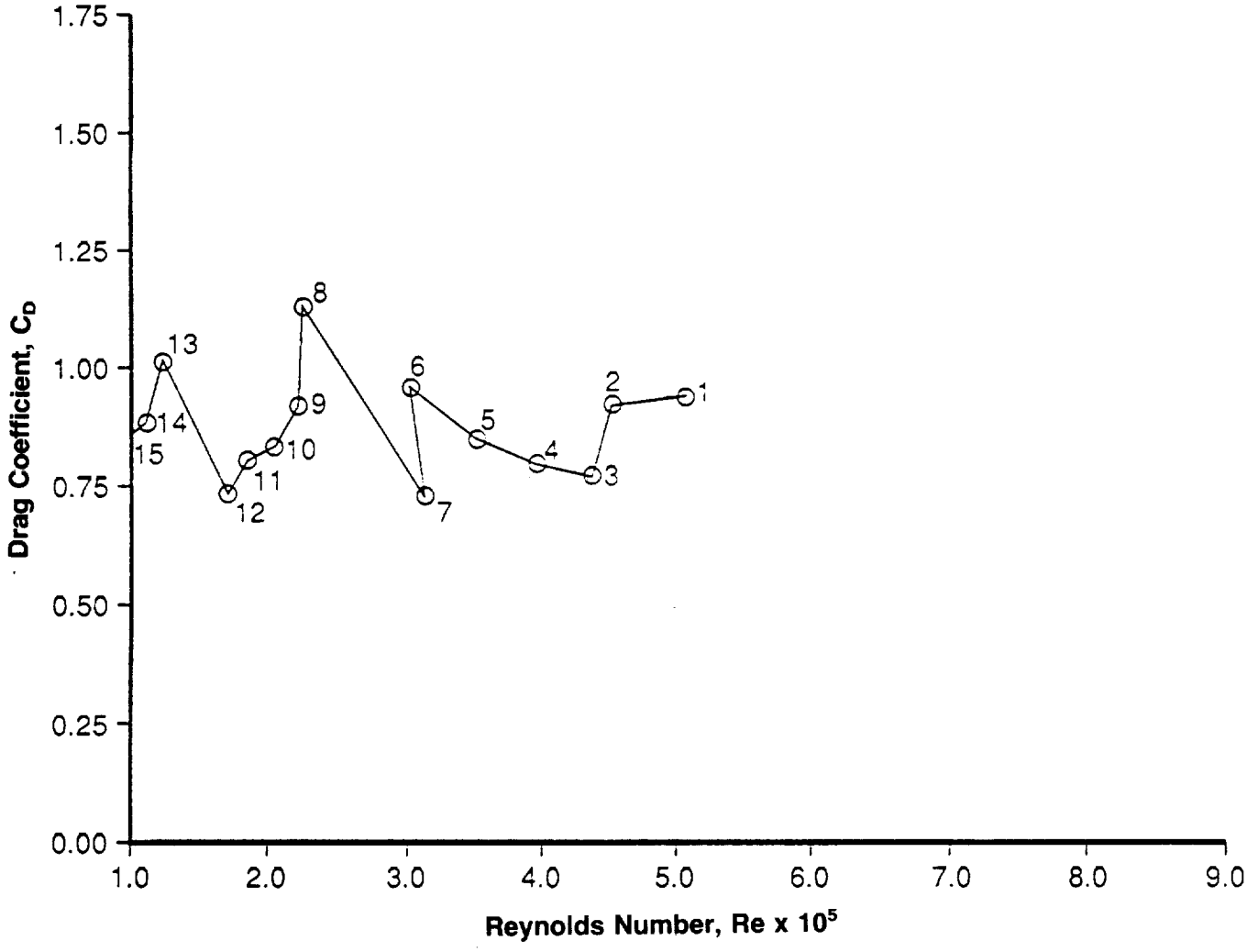

Figure 2b. C_D versus *Re* parameter obtained from FPS-16 radar/jimsphere balloon ascent during STS-13 launch, April 6, 1984 (1358Z) at KSC, Florida.

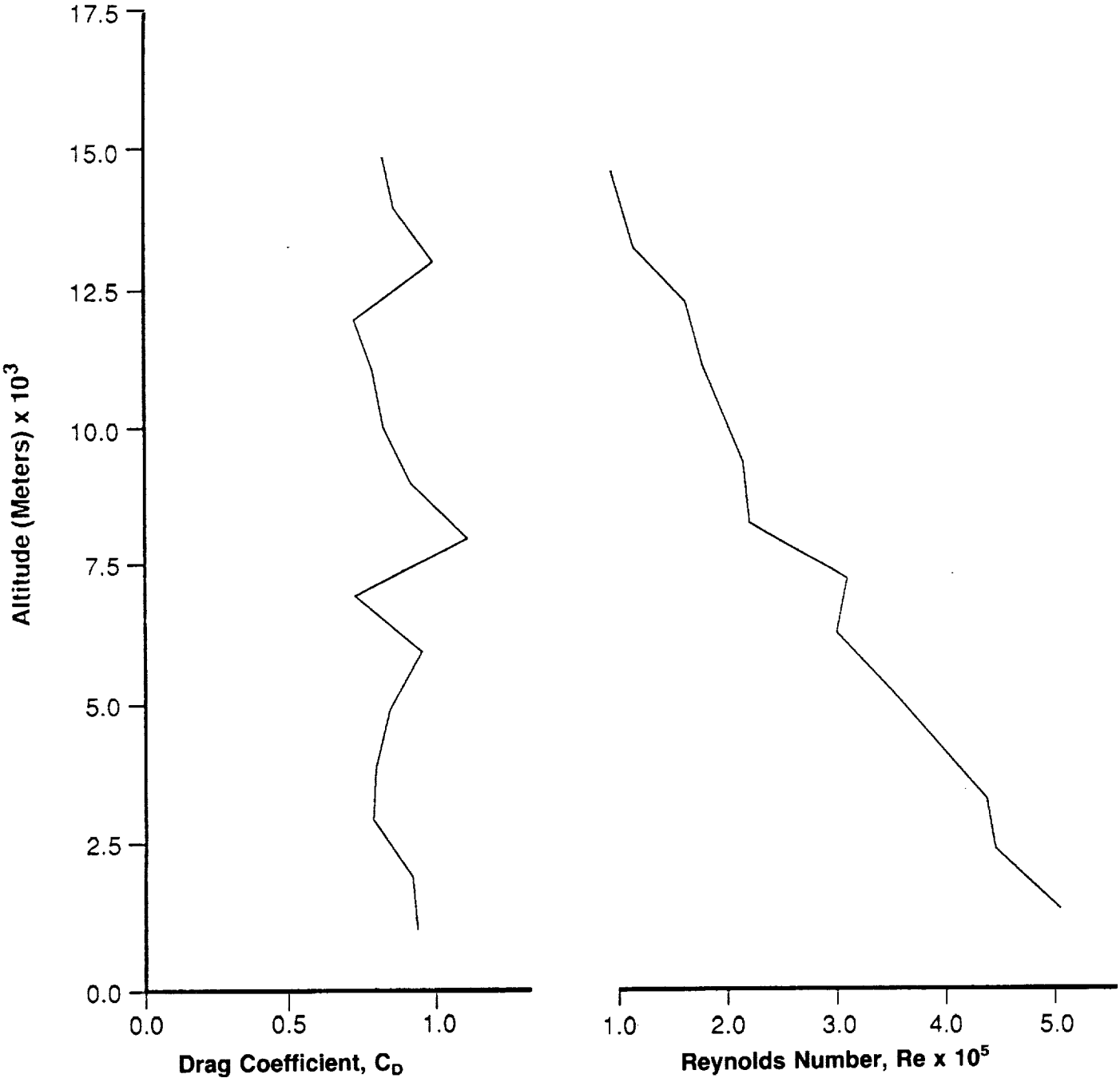

Figure 2c. C_D and *Re* altitude plots obtained from FPS-16 radar/jimsphere balloon ascent during STS-13 launch, April 6, 1984 (1358Z) at KSC, Florida.

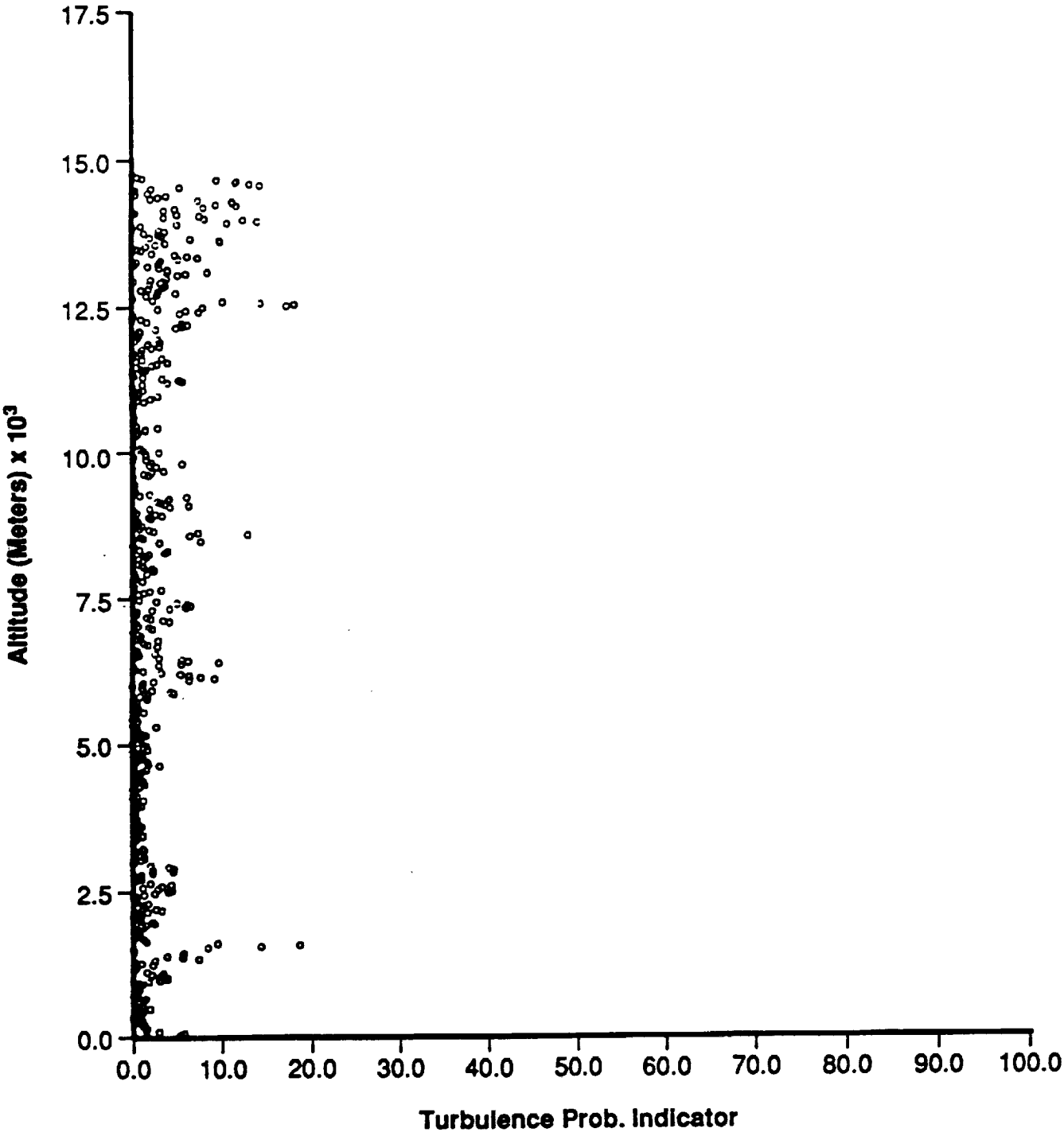

Figure 2d. Turbulence probability indicator obtained during STS-13 launch, April 6, 1984 (1358Z) at KSC, Florida.

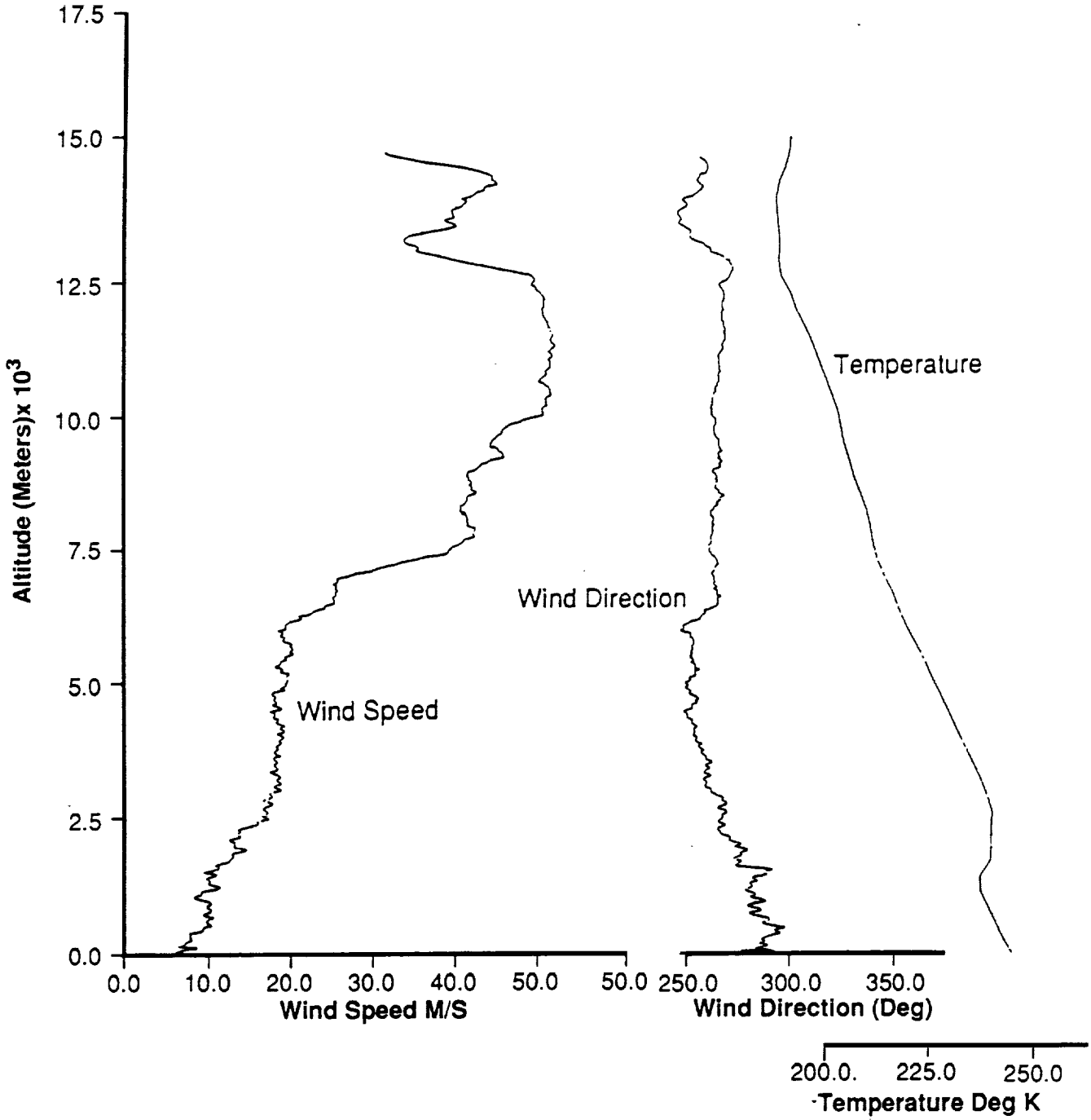

Figure 2e. Wind speed, wind direction, and temperature versus altitude plots measured during STS-13 launch, April 6, 1984 (1358Z) at KSC, Florida.

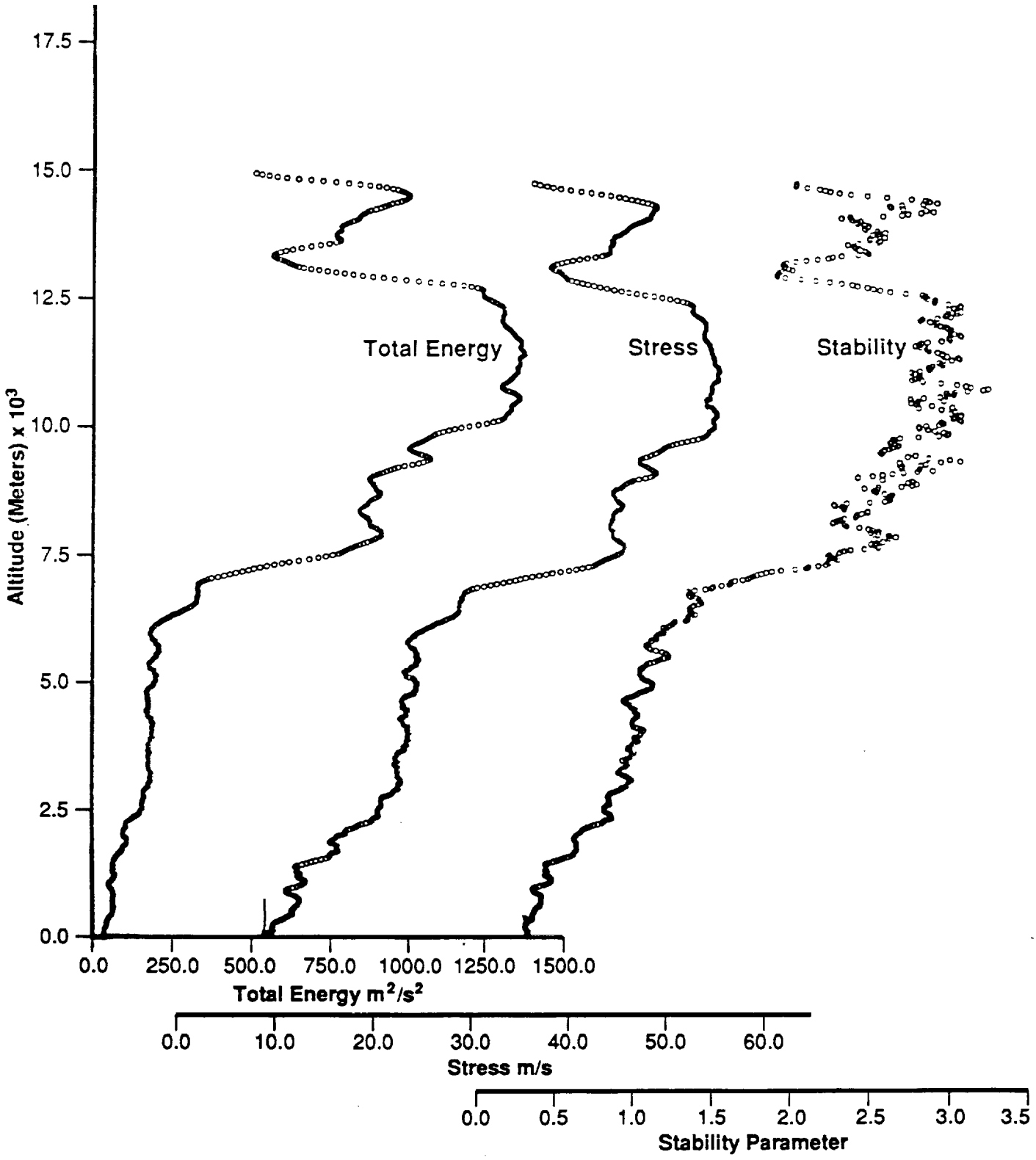

Figure 2f. Total energy, stress, and stability versus altitude parameters during STS-13 launch, April 6, 1984 (1358Z) at KSC, Florida.

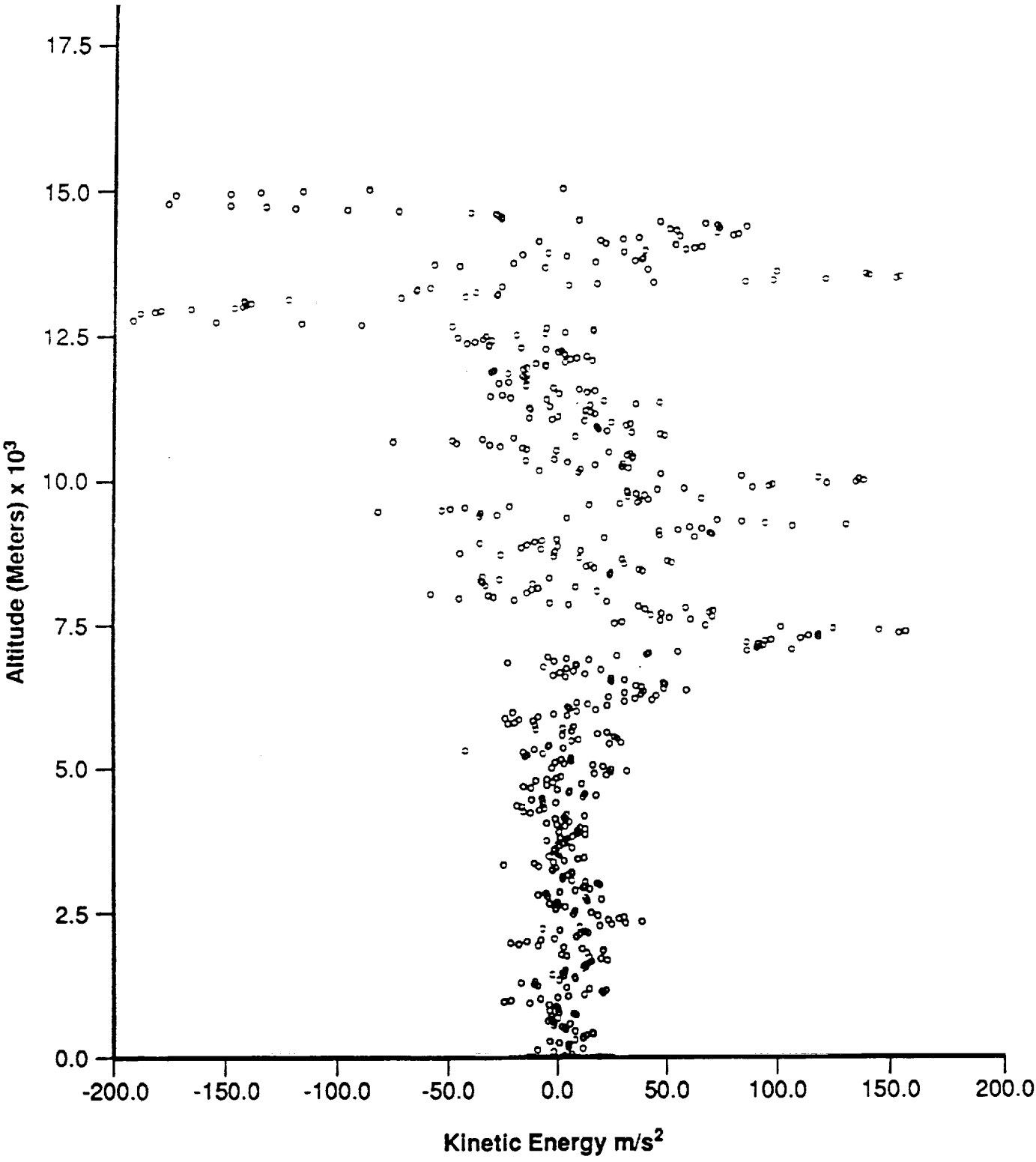

Figure 2g. Kinetic energy versus altitude parameter for STS-13 launch, April 6, 1984 (1358Z) at KSC, Florida.

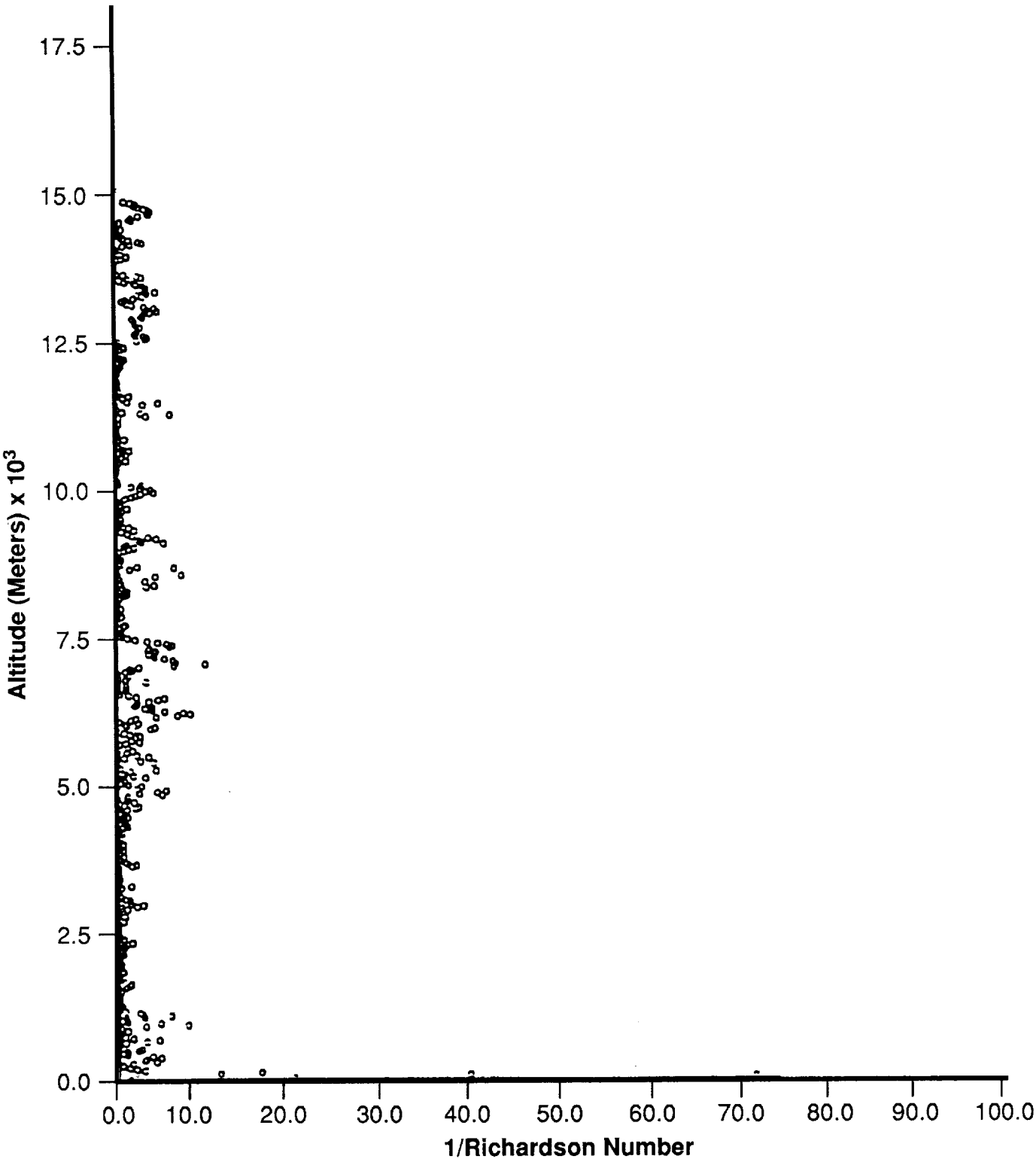

Figure 2h. Richardson number versus altitude parameter for STS-13 launch, April 6, 1984 (1358Z) at KSC, Florida.

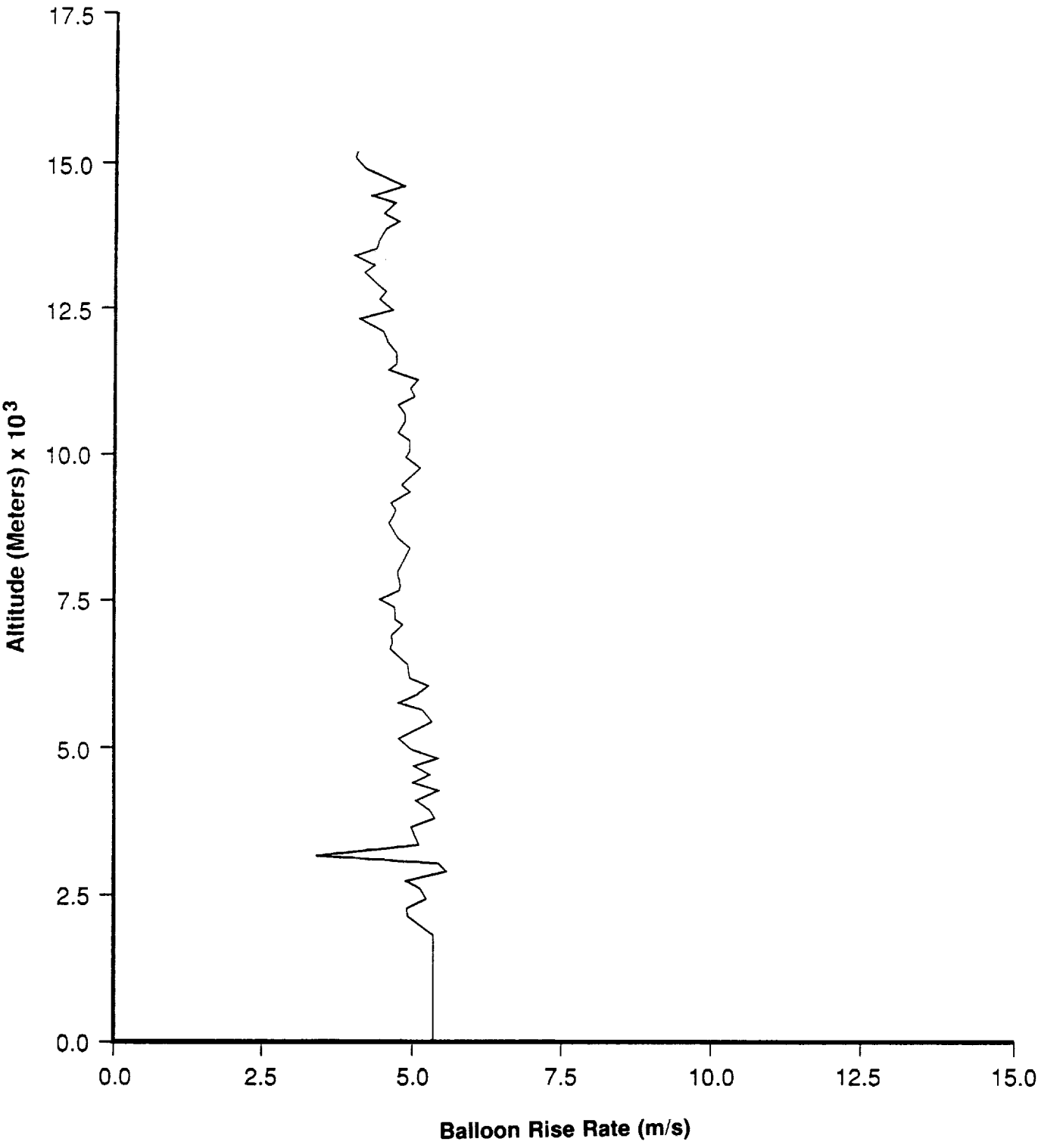

Figure 3a. Rise rate of FPS-16 radar/jimsphere balloon ascent obtained during STS-41D launch, August 30, 1984 (1242Z) at KSC, Florida.

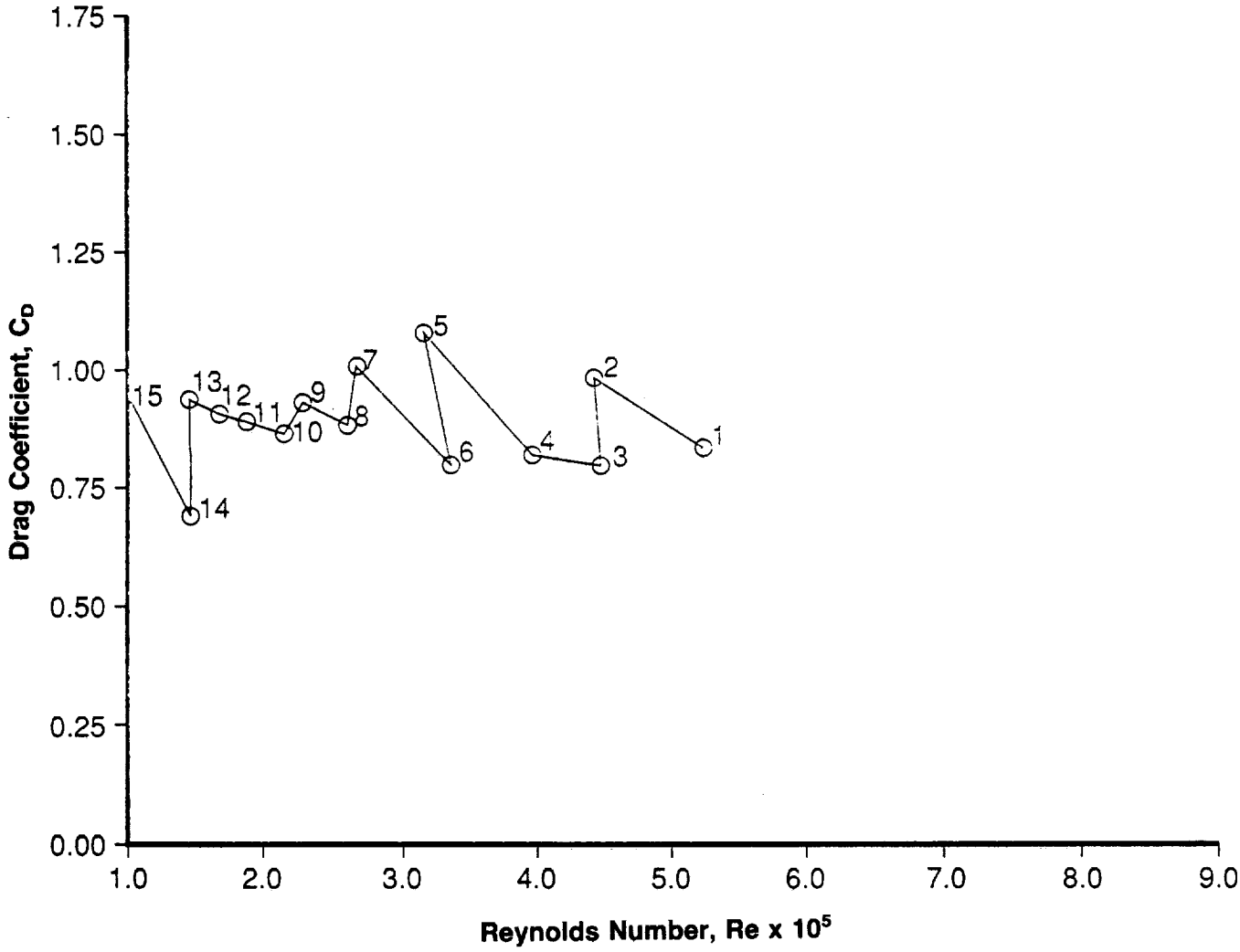

Figure 3b. C_D versus Re parameter obtained from FPS-16 radar/jimsphere balloon ascent during STS-41D launch, August 30, 1984 (1242Z) at KSC, Florida.

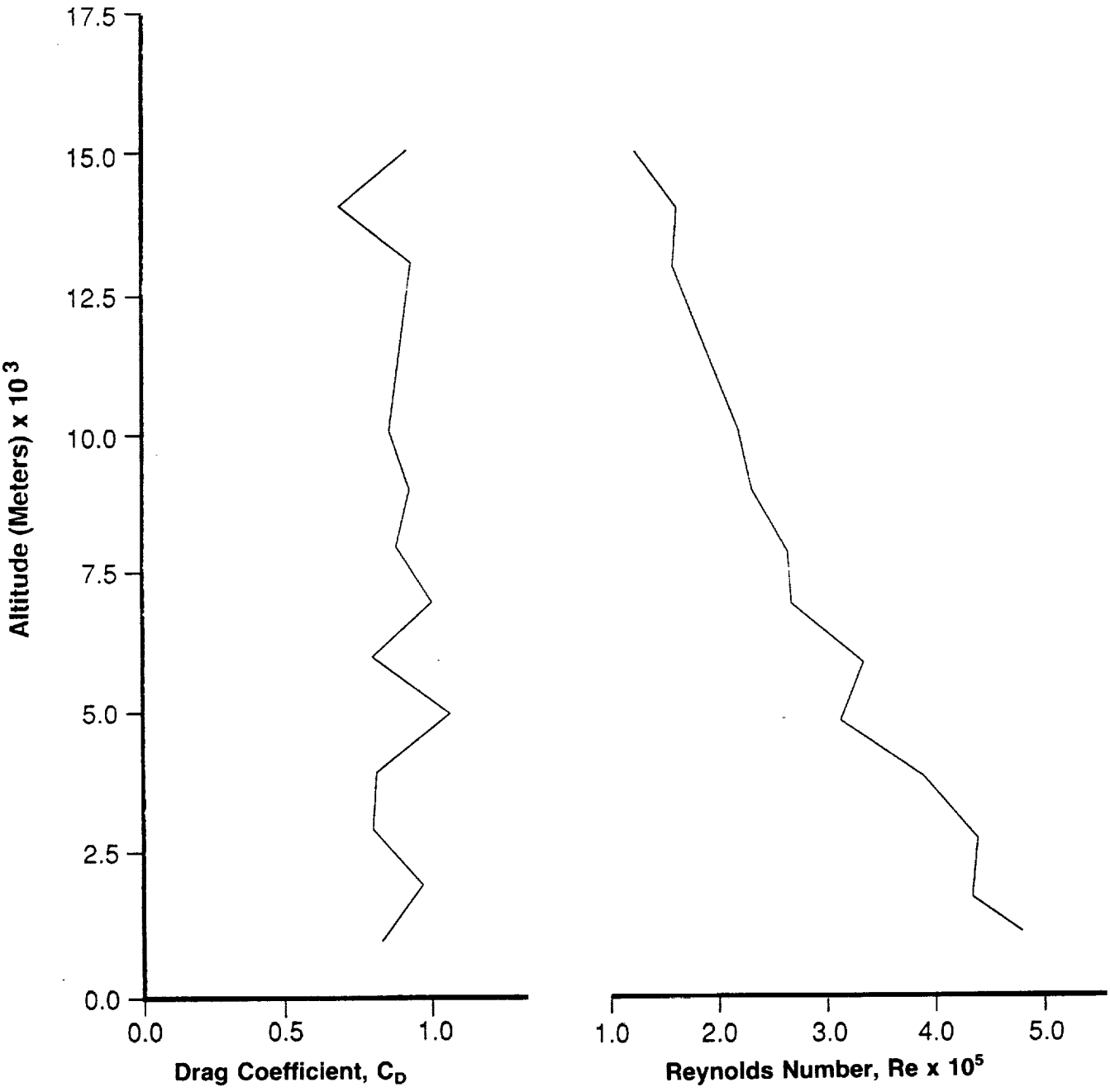

Figure 3c. C_D versus Re altitude plots obtained from FPS-16 radar/jimsphere balloon ascent during STS-41D launch, August 30, 1984 (1242Z) at KSC, Florida.

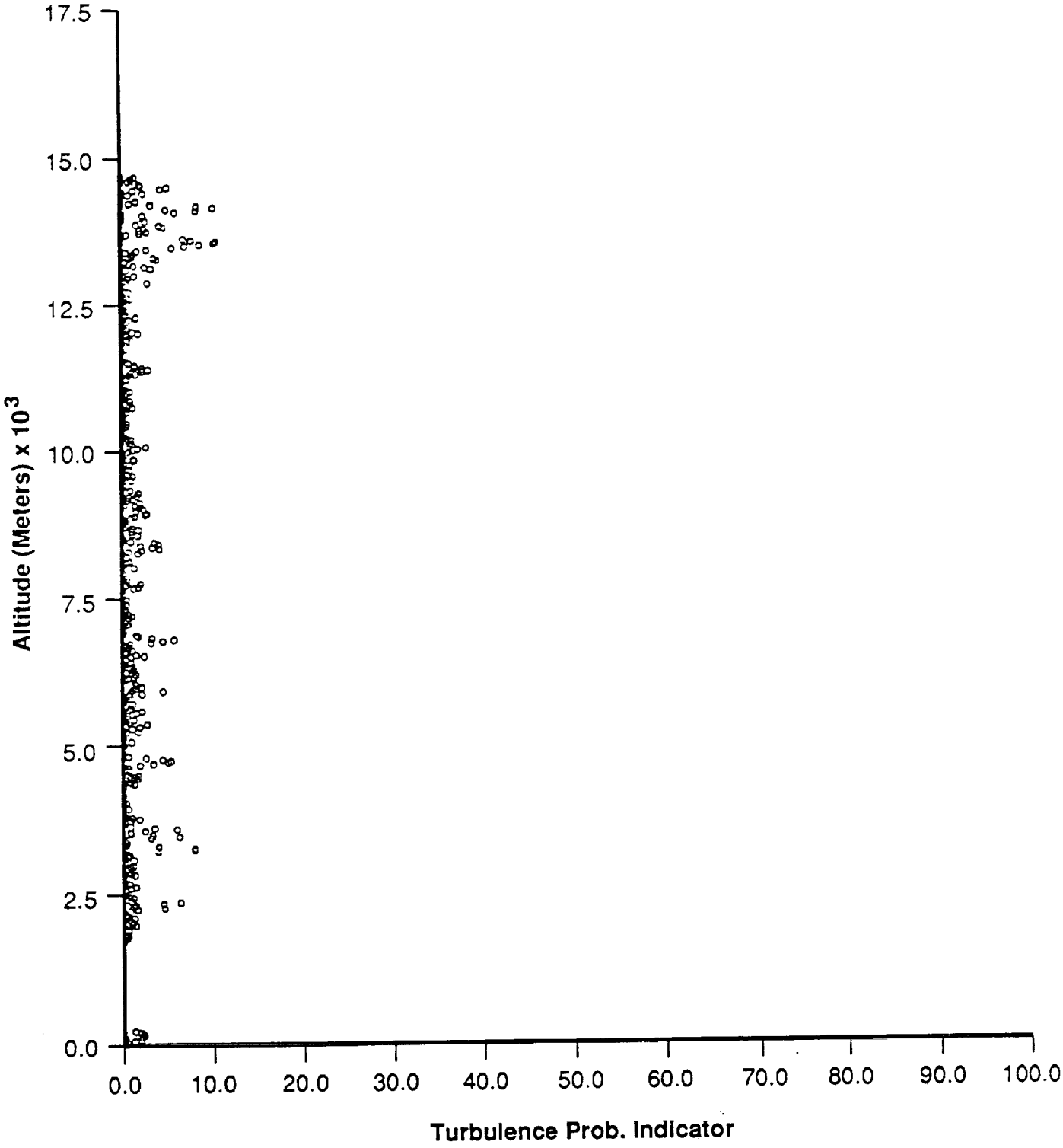

Figure 3d. Turbulence probability indicator obtained during STS-41D launch, August 30, 1984 (1242Z) at KSC, Florida.

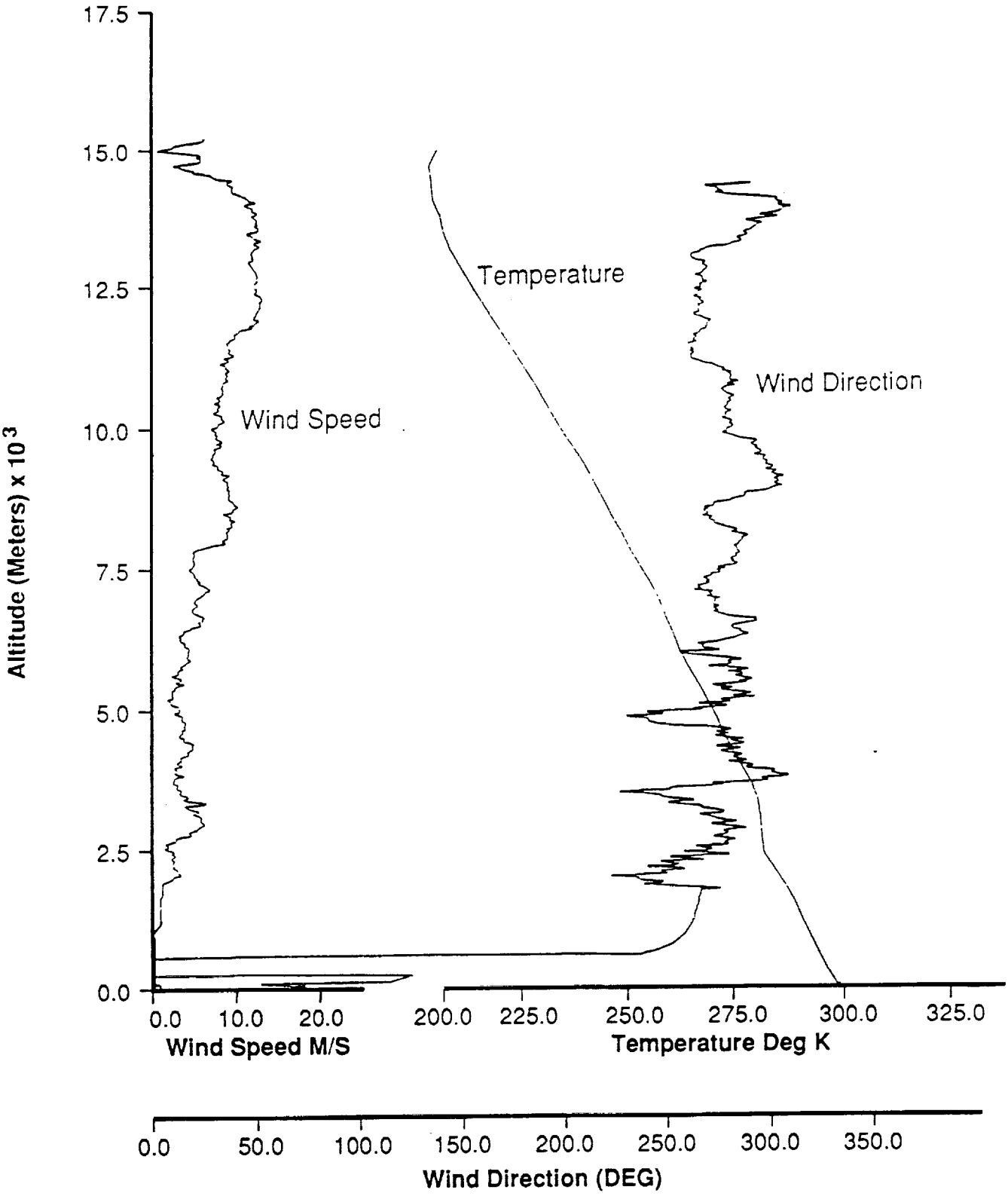

Figure 3e. Wind speed, wind direction, and temperature versus altitude plots measured during STS-41D launch, August 30, 1984 (1242Z) at KSC, Florida.

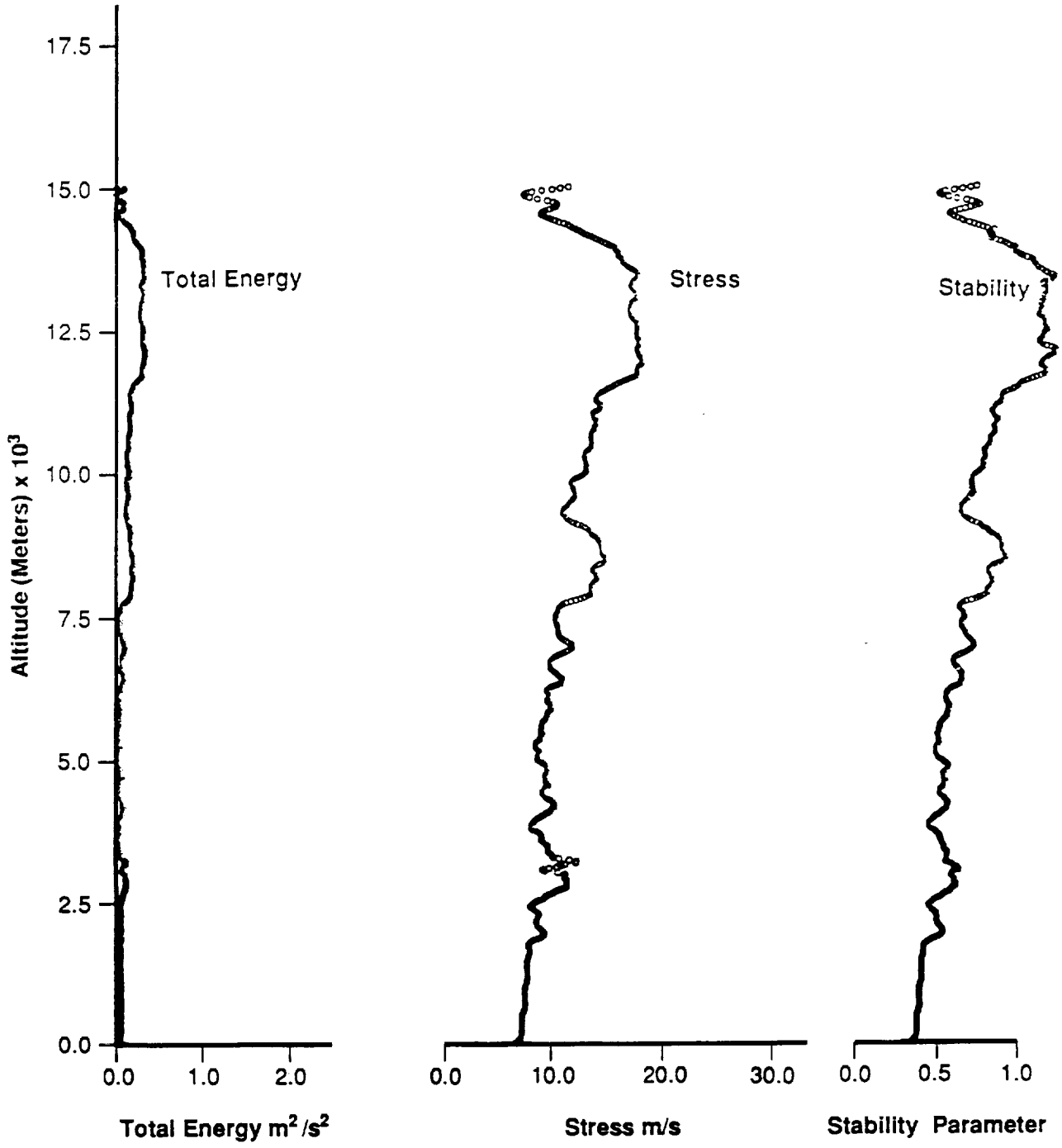

Figure 3f. Total energy, stress, and stability versus altitude parameters during STS-41D launch, August 30, 1984 (1242Z) at KSC, Florida.

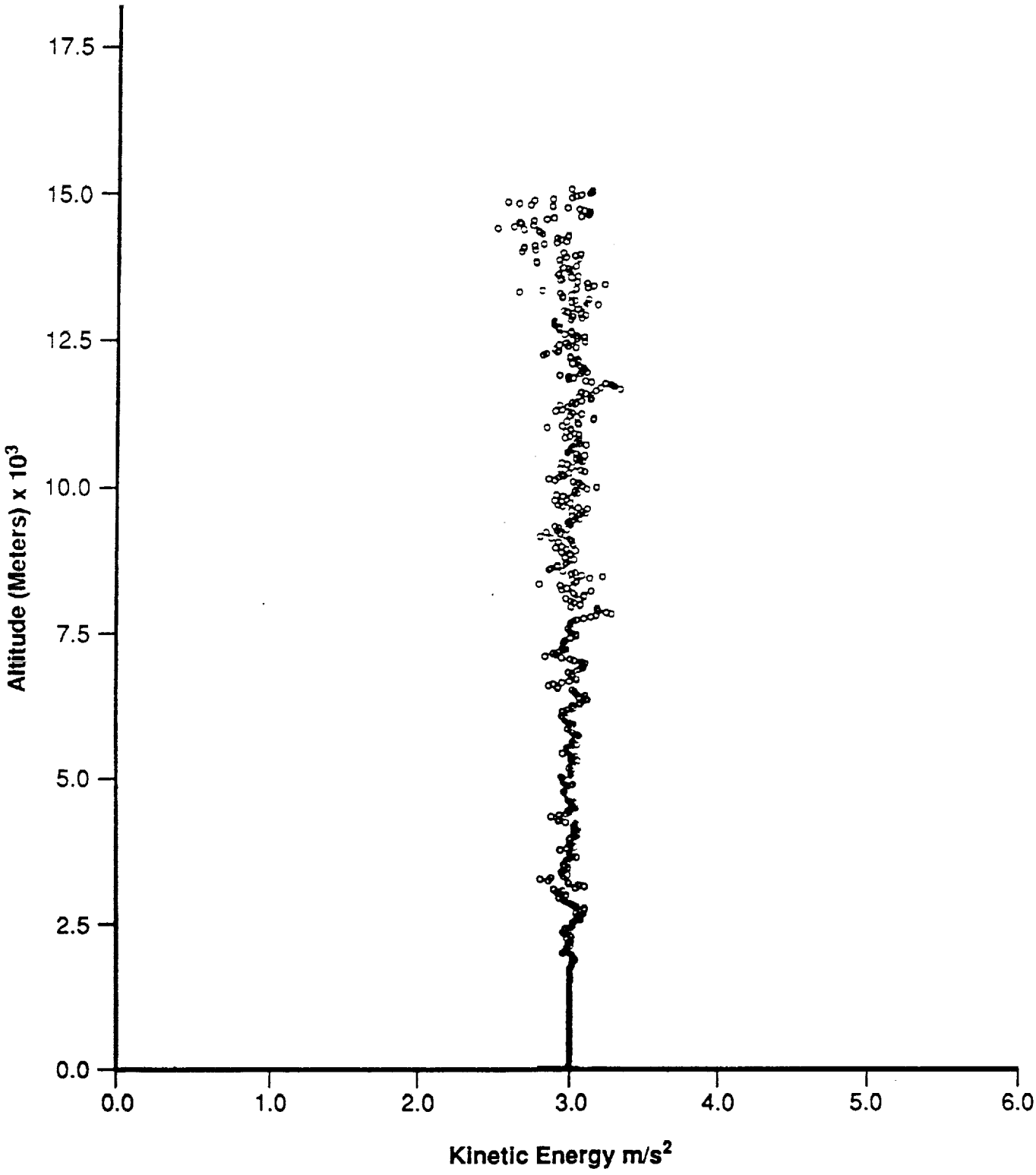

Figure 3g. Kinetic energy versus altitude parameter for STS-41D launch, August 30, 1984 (1242Z) at KSC, Florida.

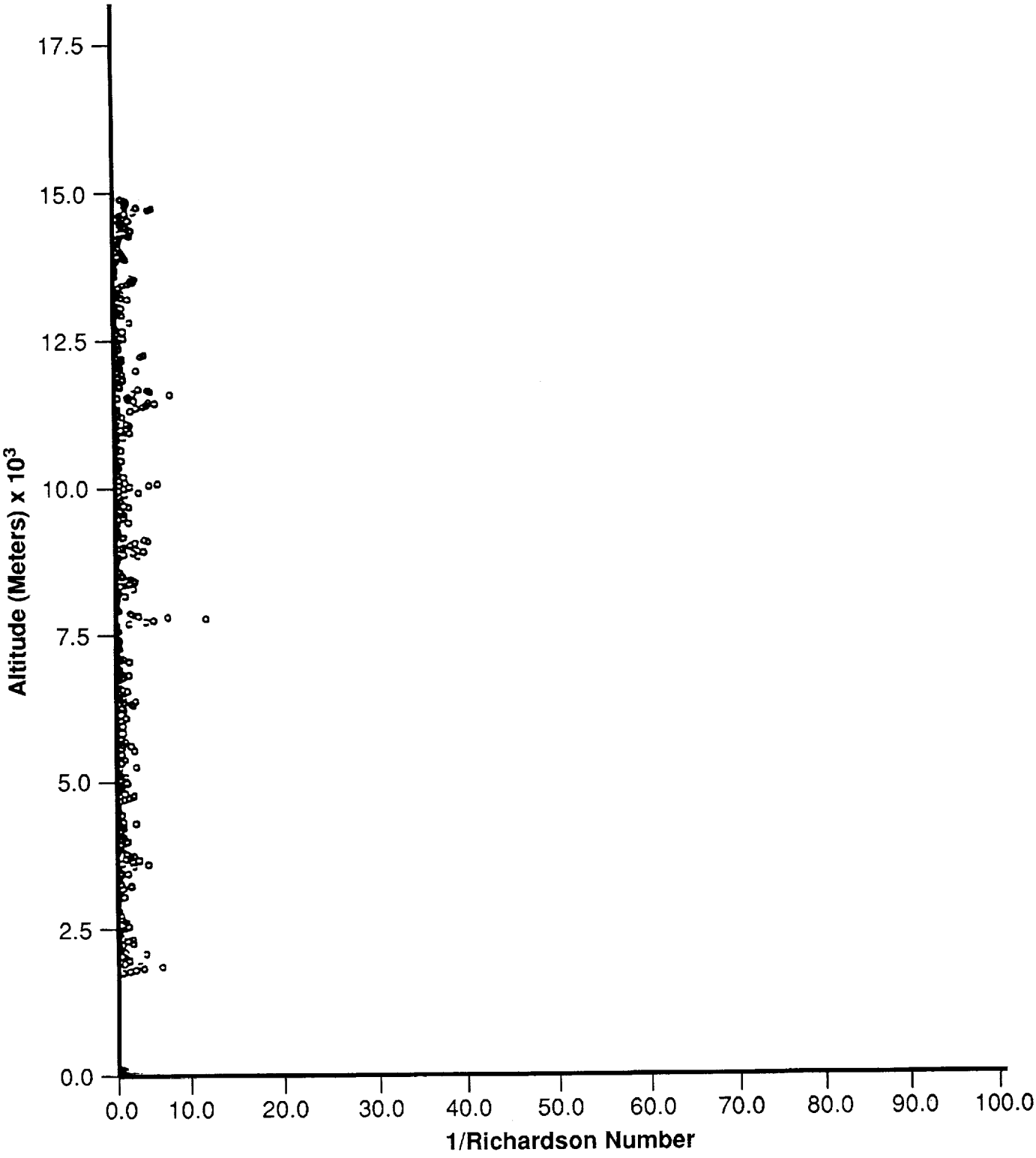

Figure 3h. Richardson number versus altitude parameter for STS-41D launch, August 30, 1984 (1242Z) at KSC, Florida.

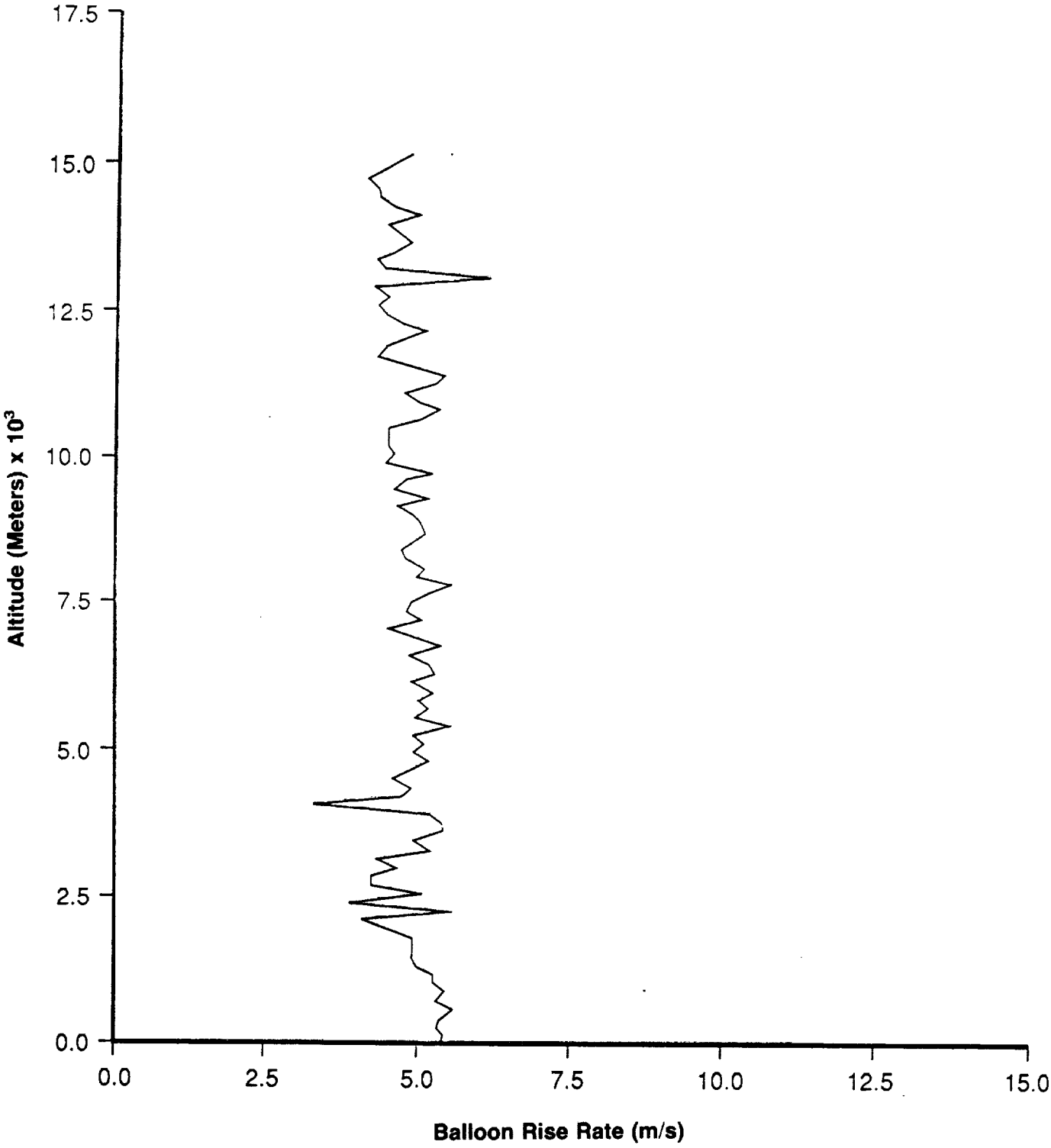

Figure 4a. Rise rate of FPS-16 radar/jimsphere balloon ascent obtained during STS-51D launch, April 12, 1985 (1359Z) at KSC, Florida.

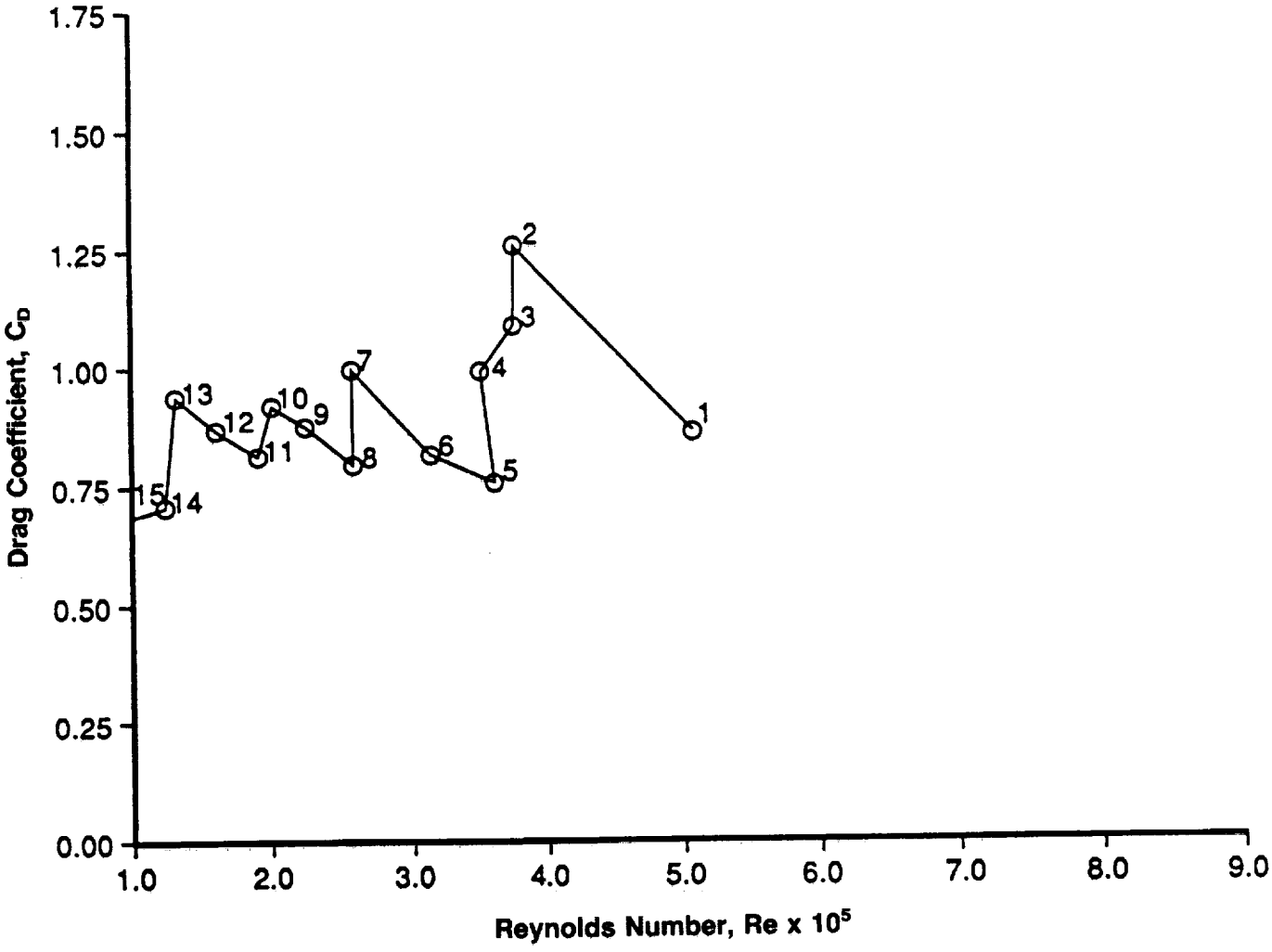

Figure 4b. C_D versus *Re* parameter obtained from FPS-16 radar/jimsphere balloon ascent during STS-51D launch, April 12, 1985 (1359Z) at KSC, Florida.

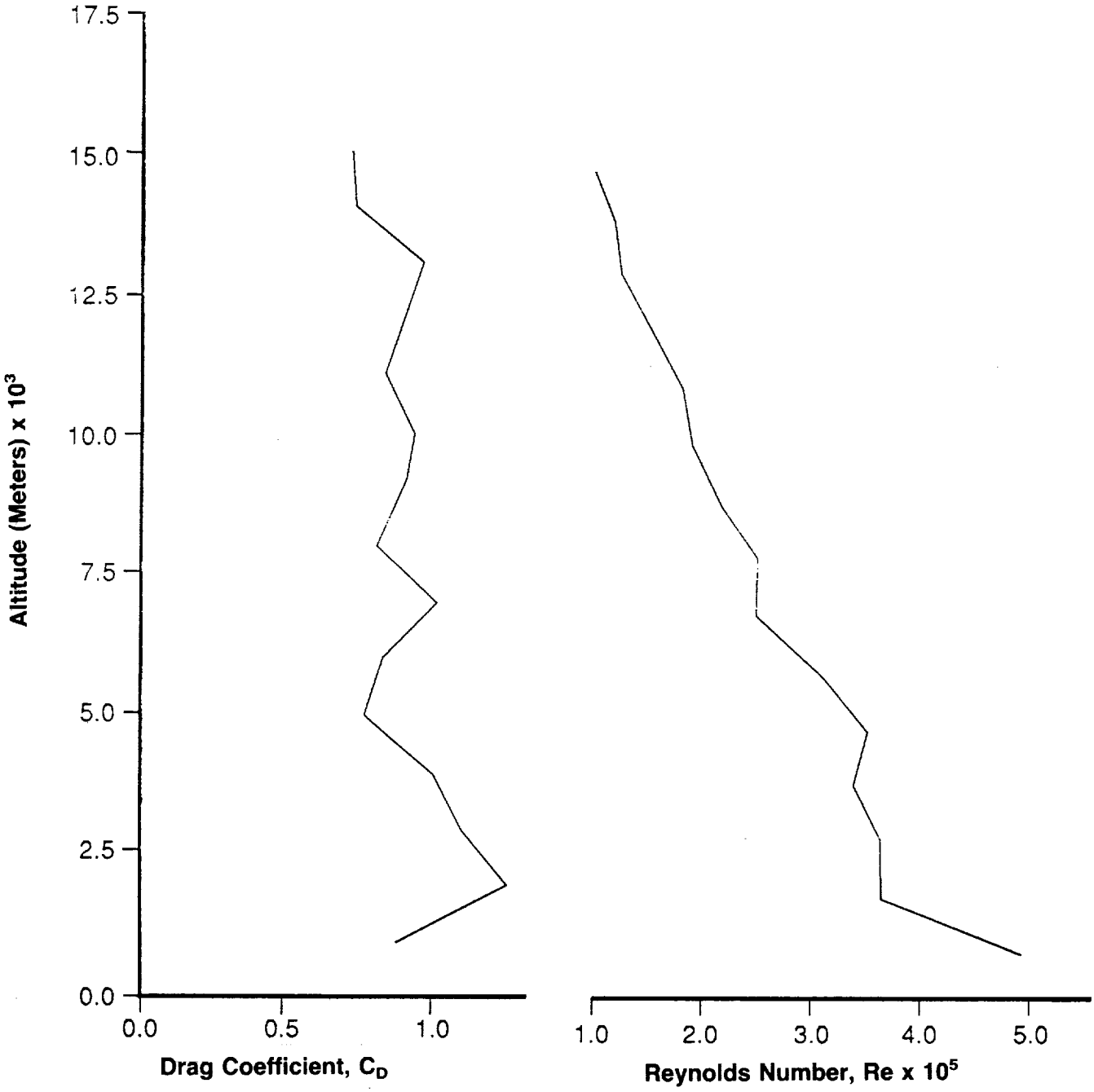

Figure 4c. C_D and *Re* versus altitude plots obtained from FPS-16 radar/jimsphere balloon ascent during STS-51D launch, April 12, 1985 (1359Z) at KSC, Florida.

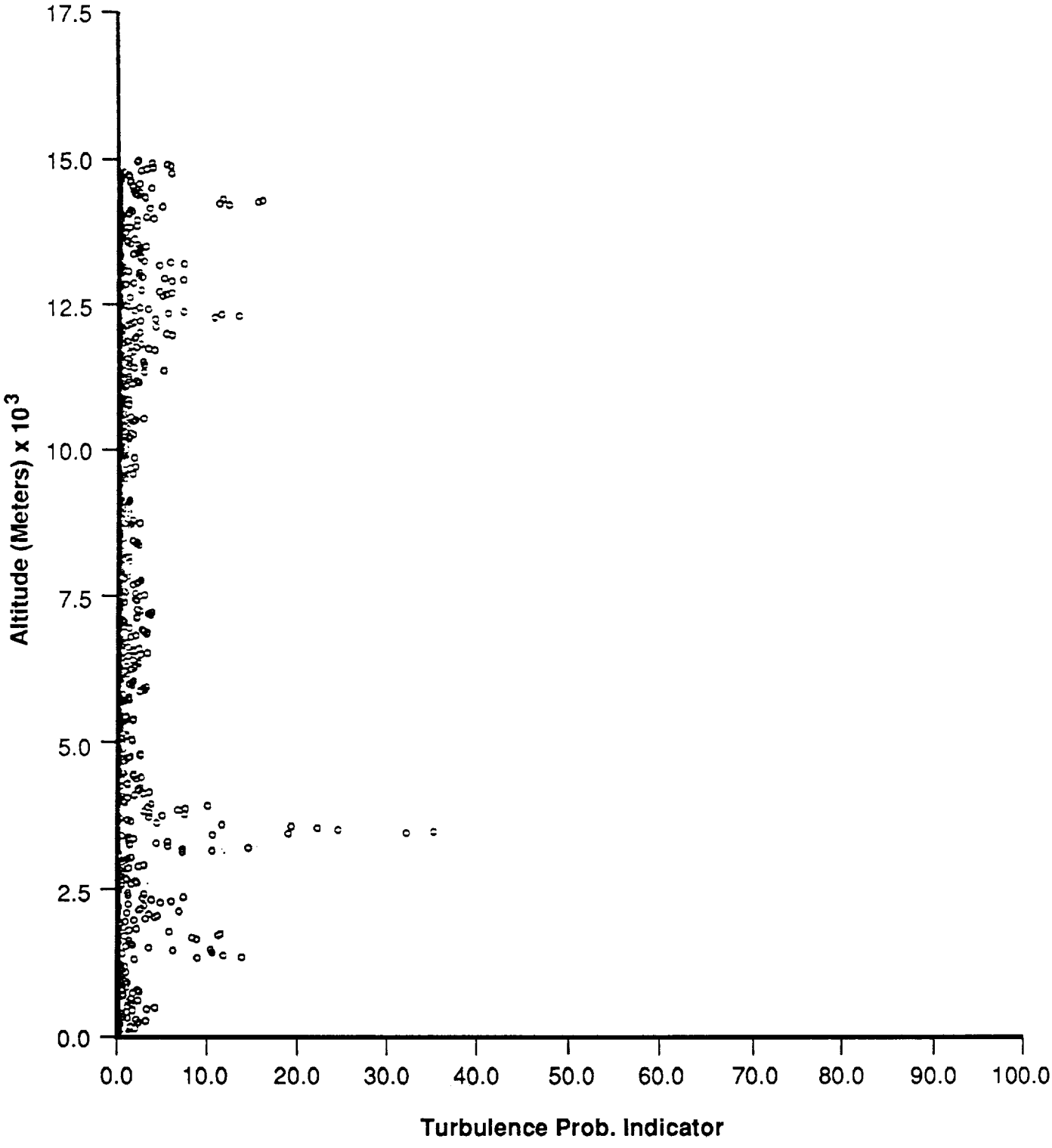

Figure 4d. Turbulence probability indicator obtained during STS-51D launch, April 12, 1985 (1359Z) at KSC, Florida.

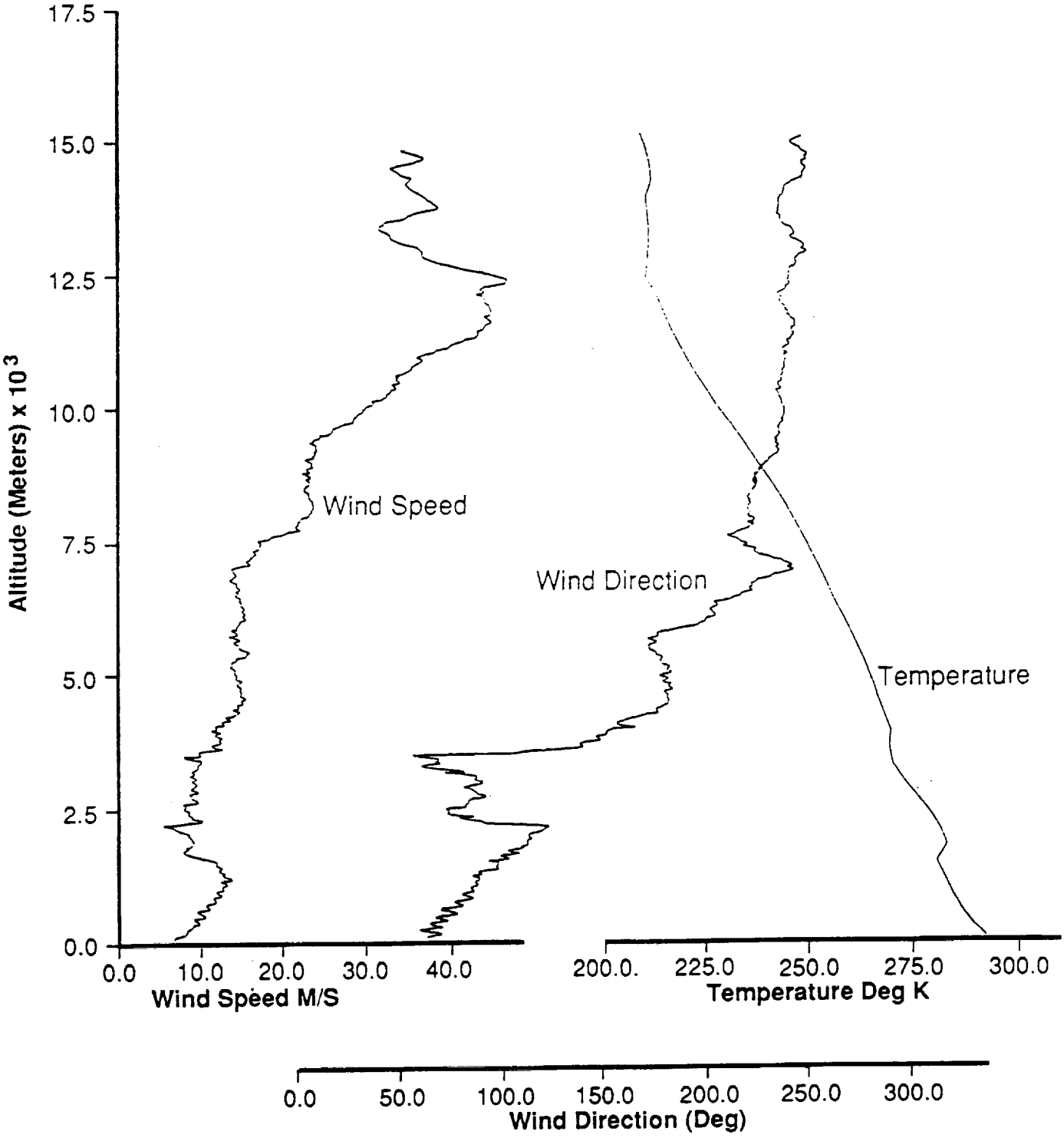

Figure 4e. Wind speed, wind direction, and temperature versus altitude plots measured during STS-51D launch, April 12, 1985 (1359Z) at KSC, Florida.

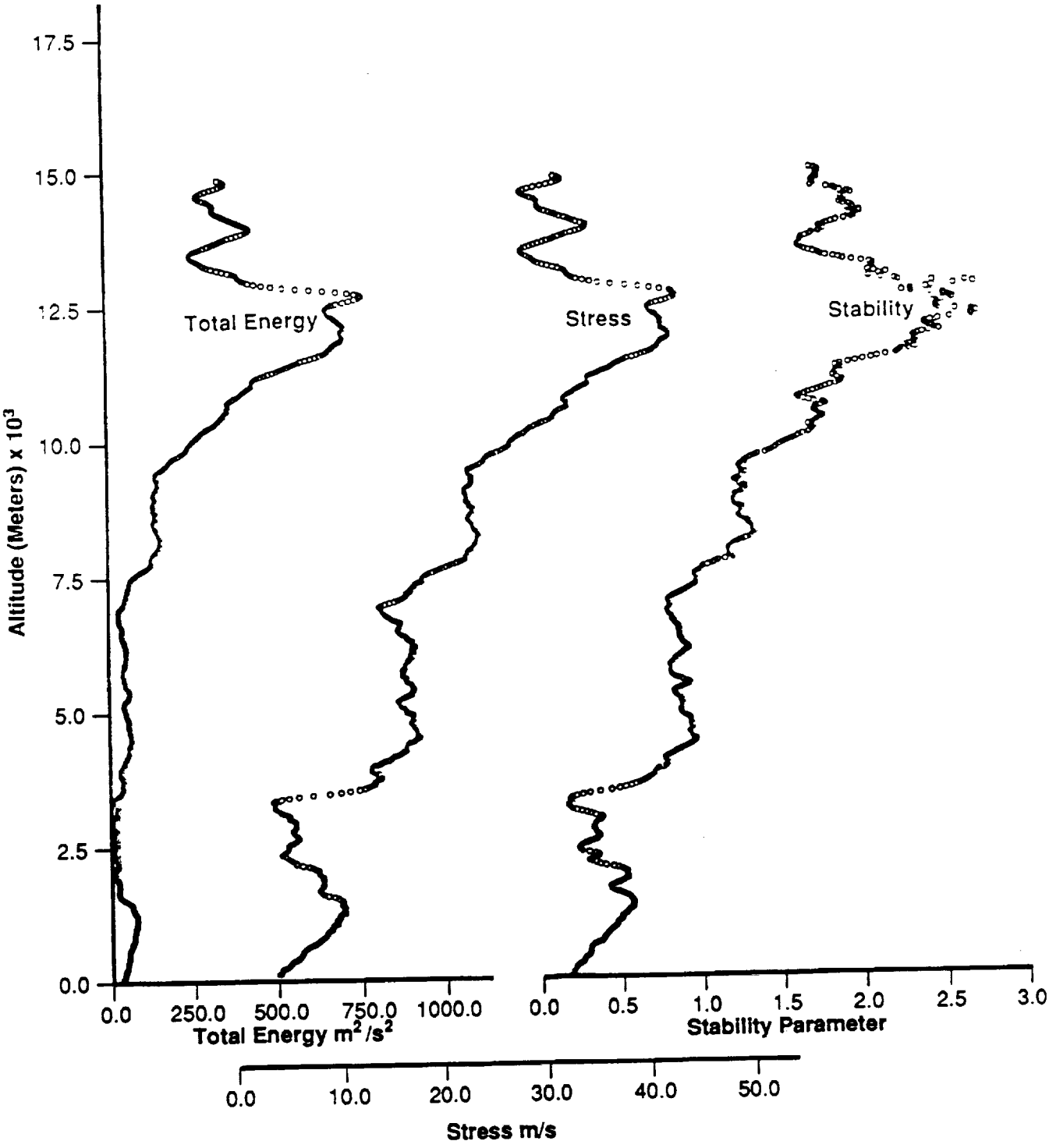

Figure 4f. Total energy, stress, and stability parameters versus altitude for STS-51D launch, April 12, 1985 (1359Z) at KSC, Florida.

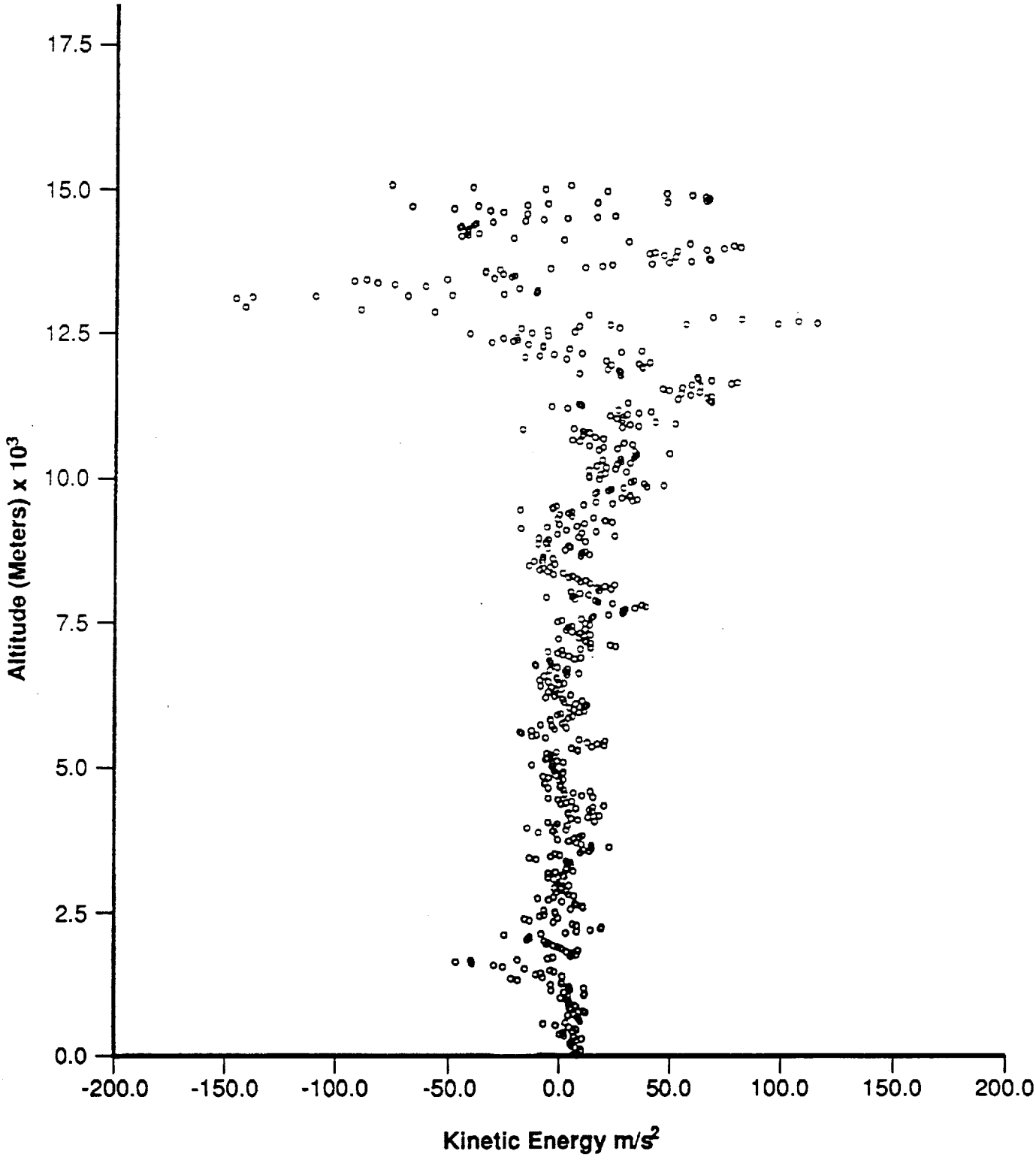

Figure 4g. Kinetic energy versus altitude parameters for STS-51D launch, April 12, 1985 (1359Z) at KSC, Florida.

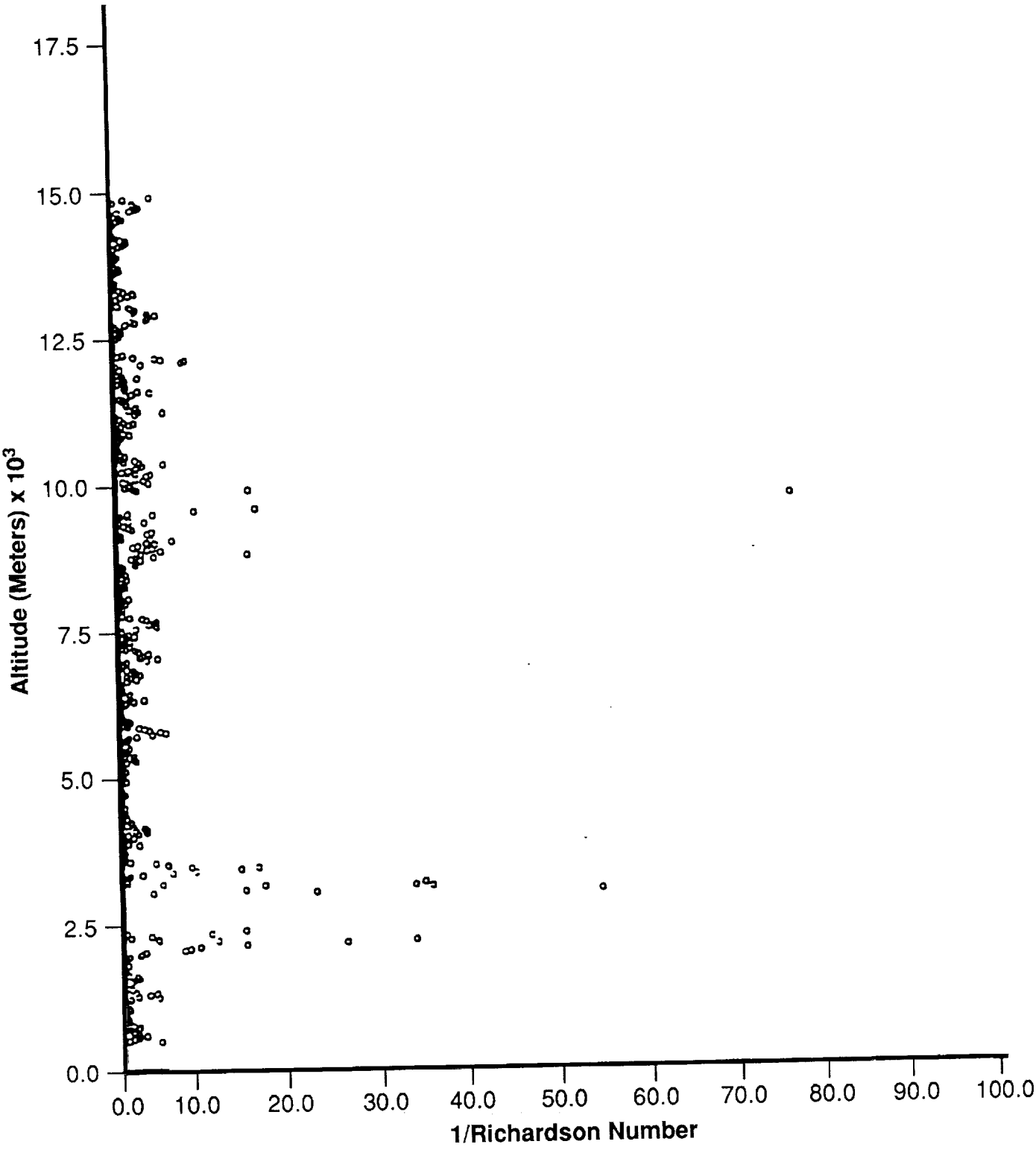

Figure 4h. Richardson number versus altitude parameters for STS-51D launch, April 12, 1985 (1359Z) at KSC, Florida.

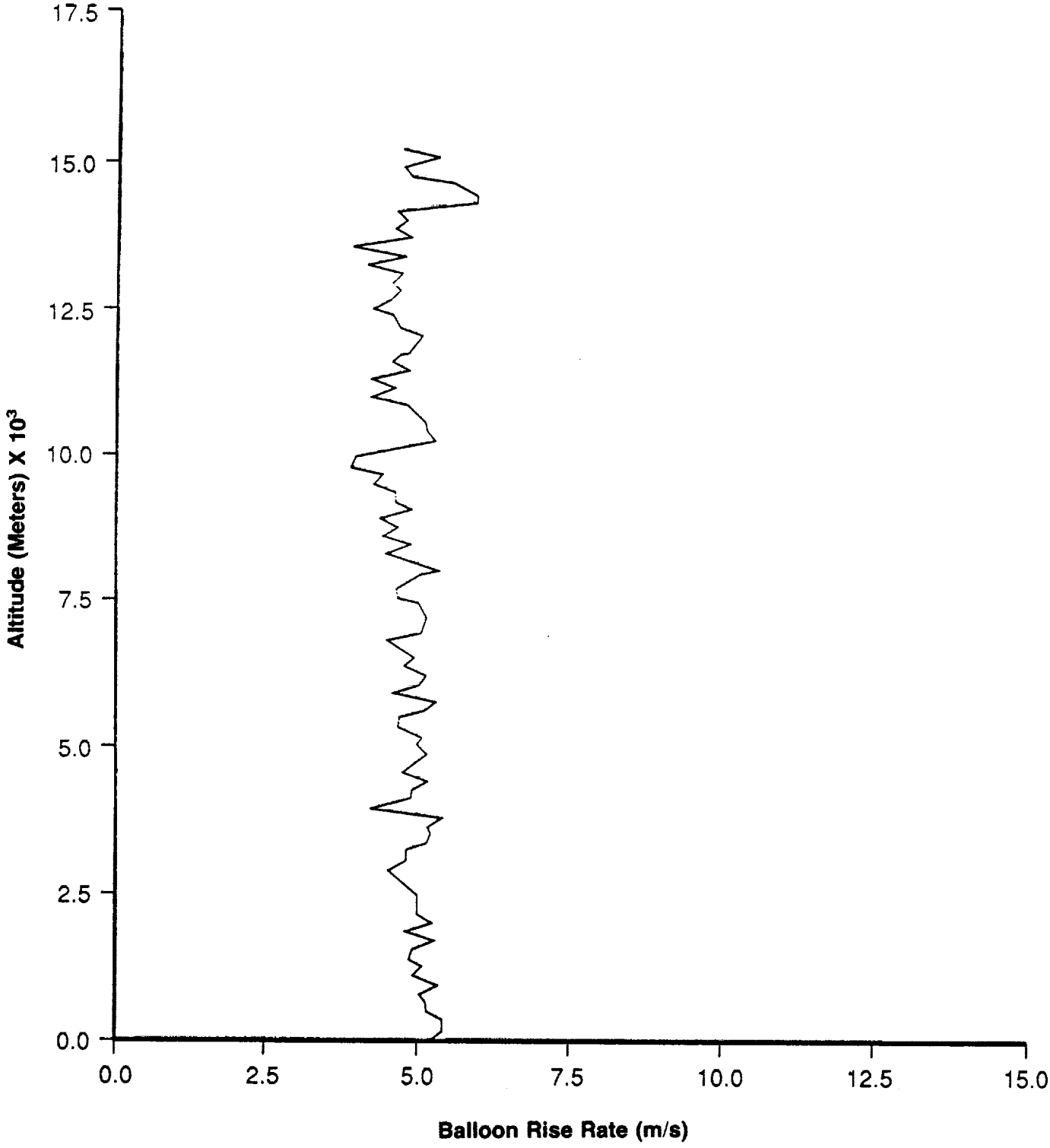

Figure 5a. Rise rate of FPS-16 radar/jimsphere balloon ascent obtained during STS-51G launch, June 17, 1985 (1133Z) at KSC, Florida.

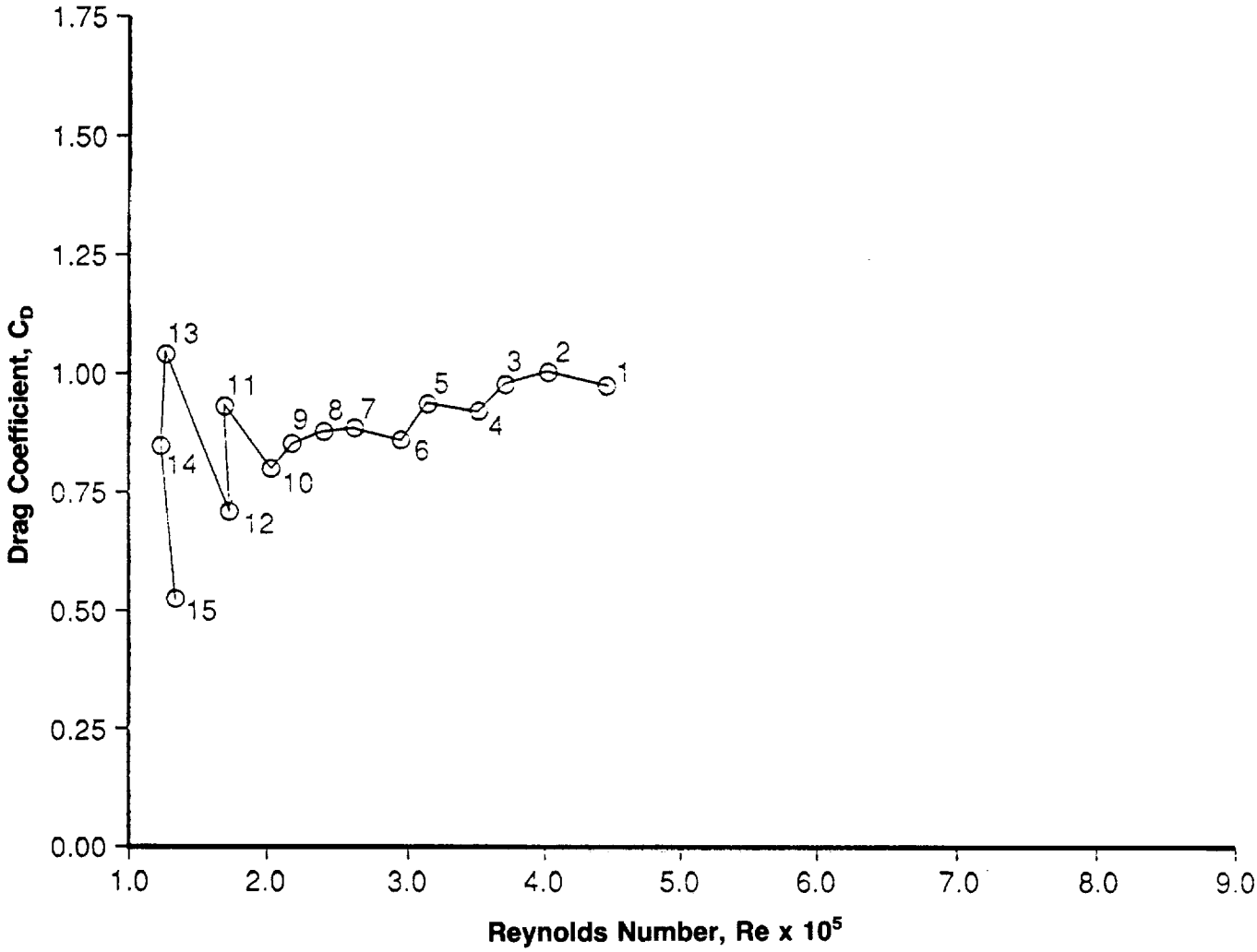

Figure 5b. C_D versus *Re* parameter obtained from FPS-16 radar/jimsphere balloon ascent during STS-51G launch, June 17, 1985 (1133Z) at KSC, Florida.

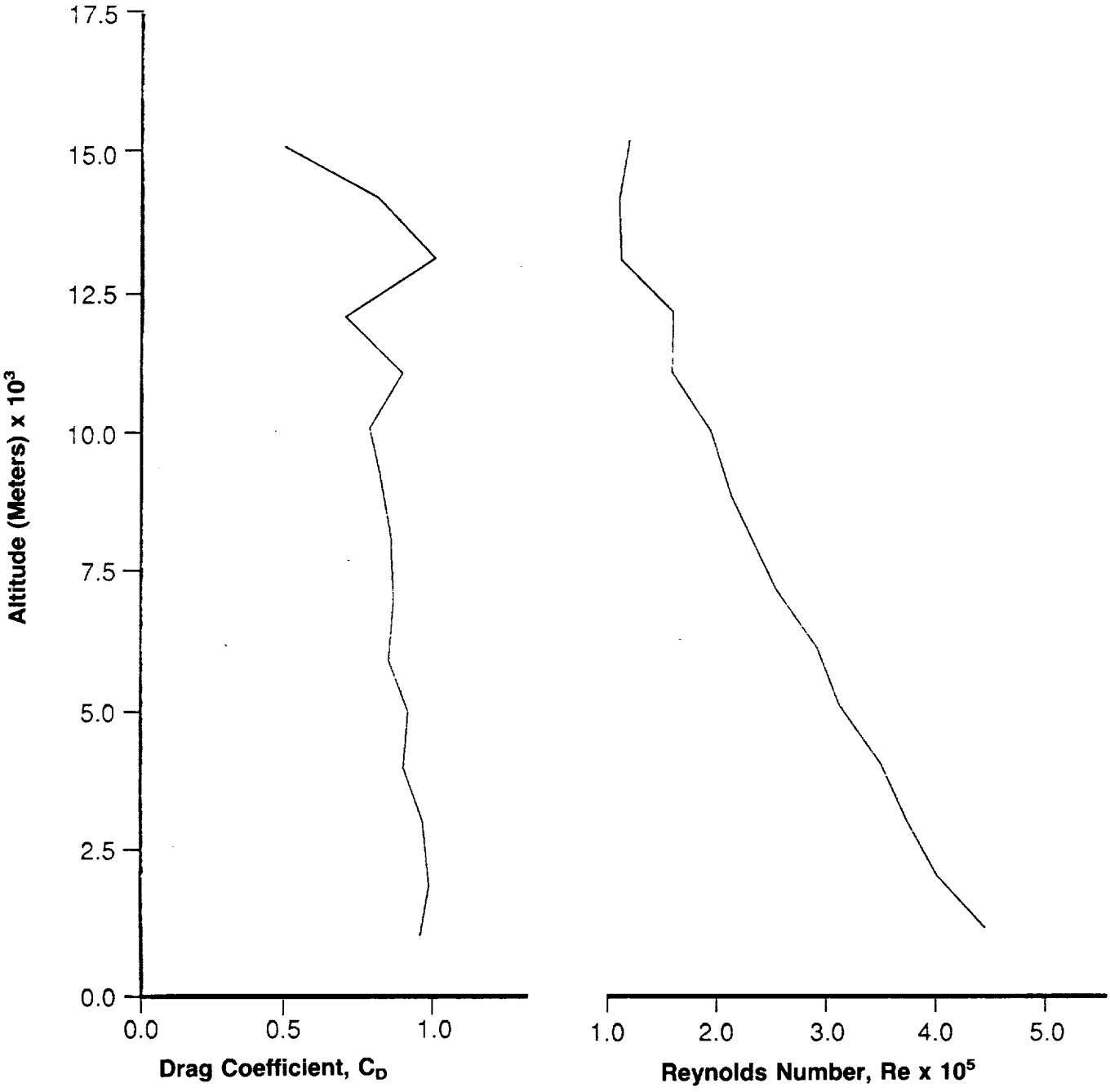

Figure 5c. C_D and *Re* altitude plots obtained from FPS-16 radar/jimsphere balloon ascent during STS-51G launch, June 17, 1985 (1133Z) at KSC, Florida.

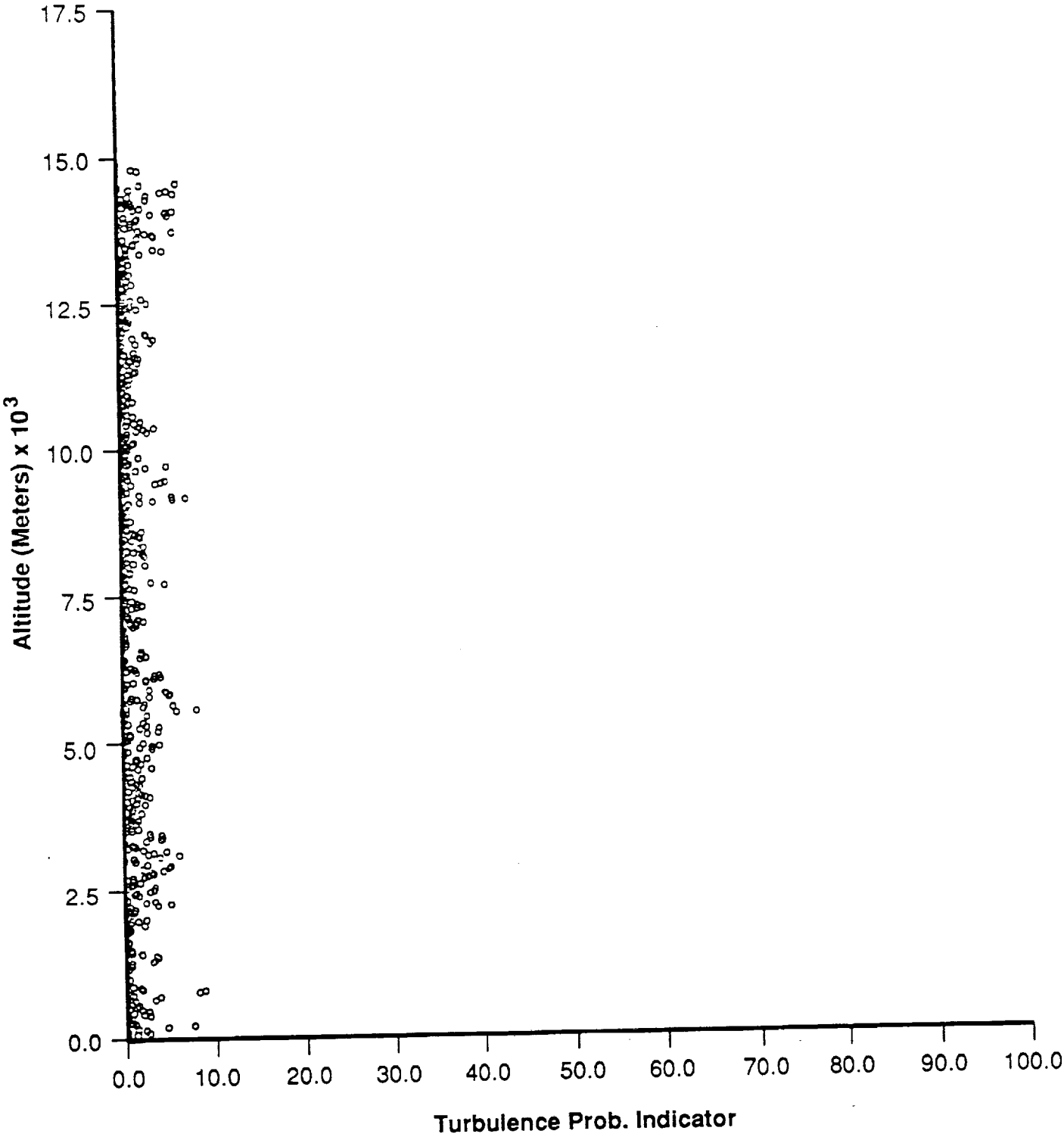

Figure 5d. Turbulence probability indicator obtained during STS-51G launch, June 17, 1985 (1133Z) at KSC, Florida.

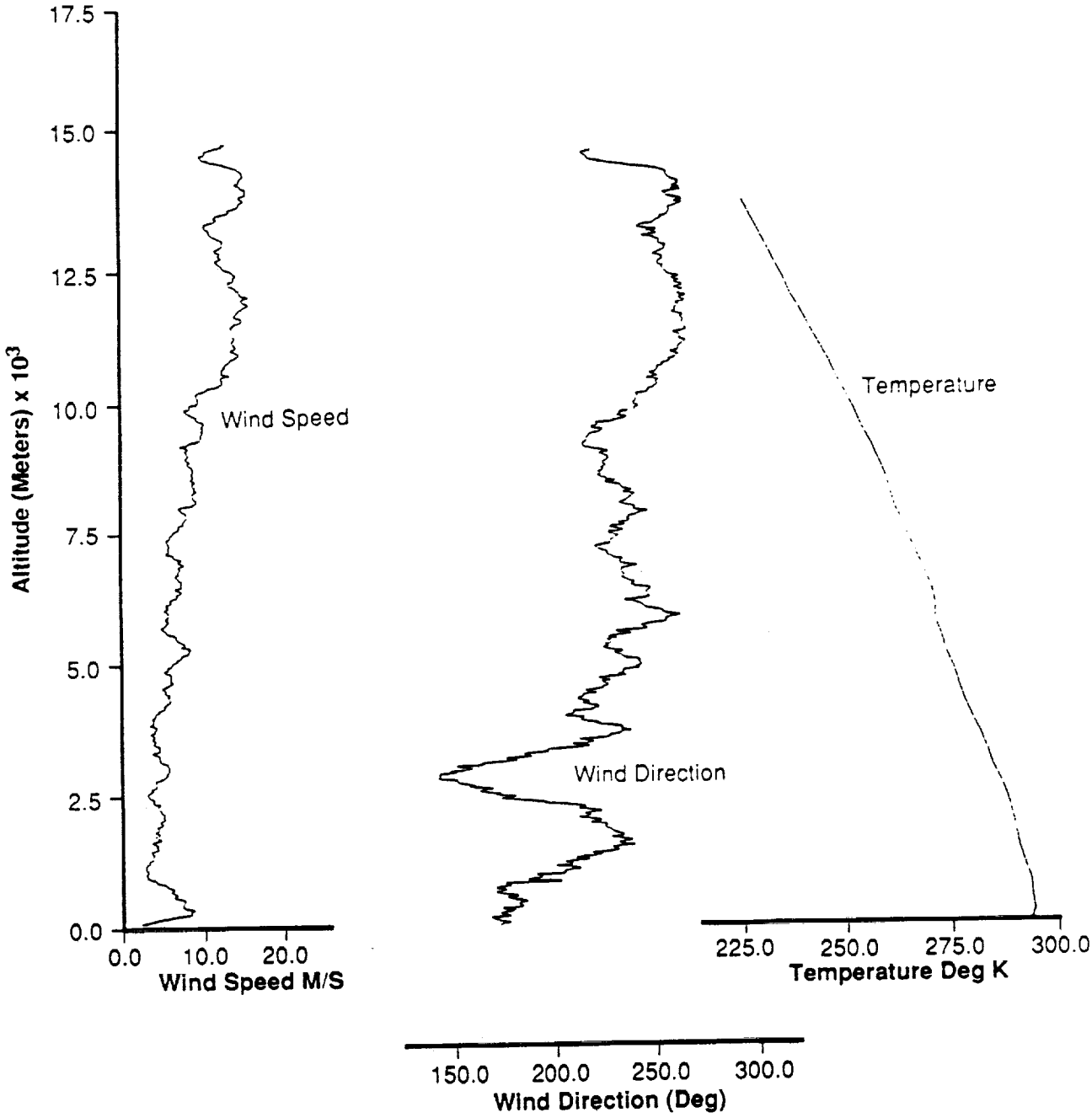

Figure 5e. Wind speed, wind direction, and temperature versus altitude plots measured during STS-51G launch, June 17, 1985 (1133Z) at KSC, Florida.

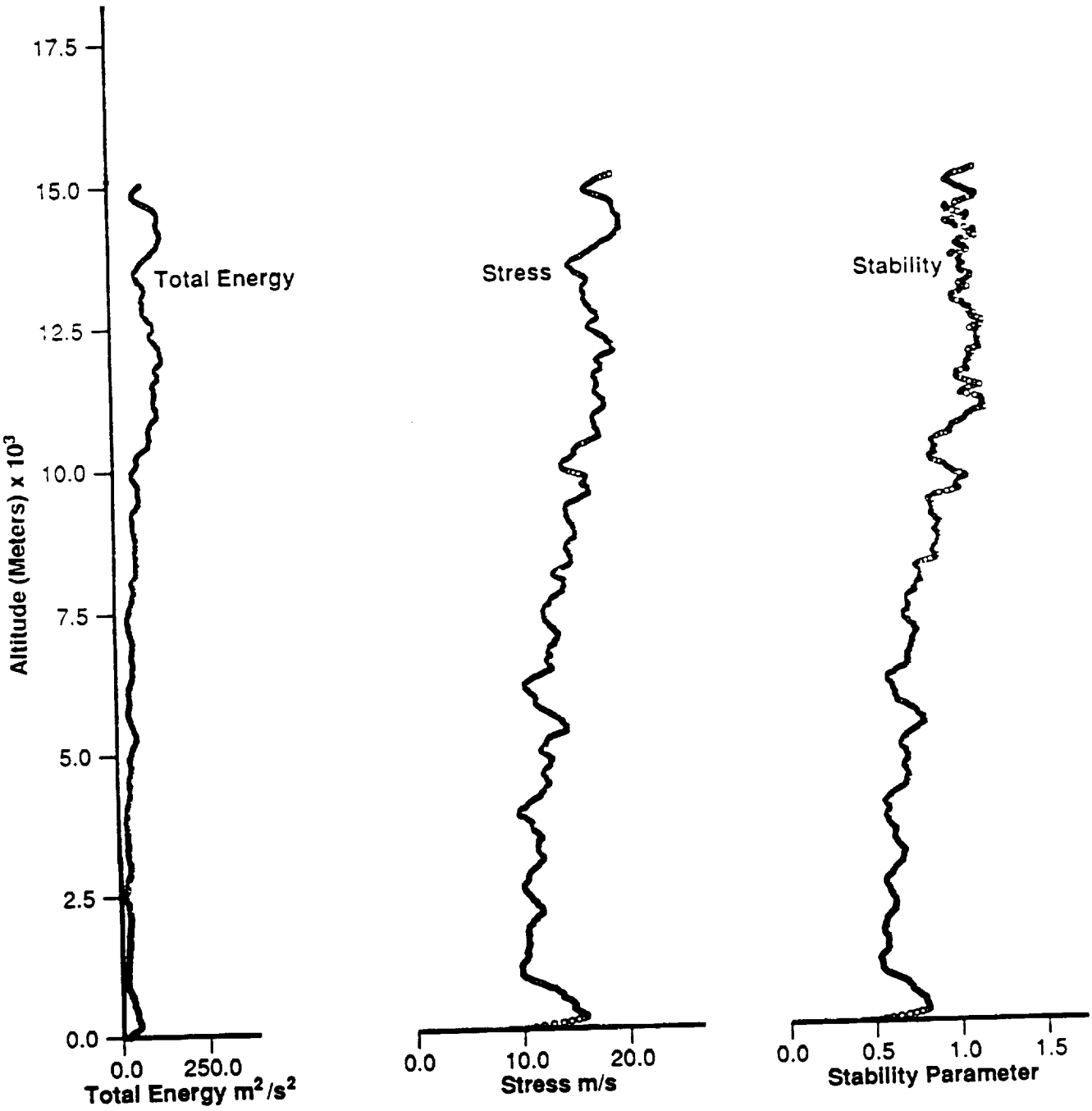

Figure 5f. Total energy, stress, and stability versus altitude parameters for STS-51G launch, June 17, 1985 (1133Z) at KSC, Florida.

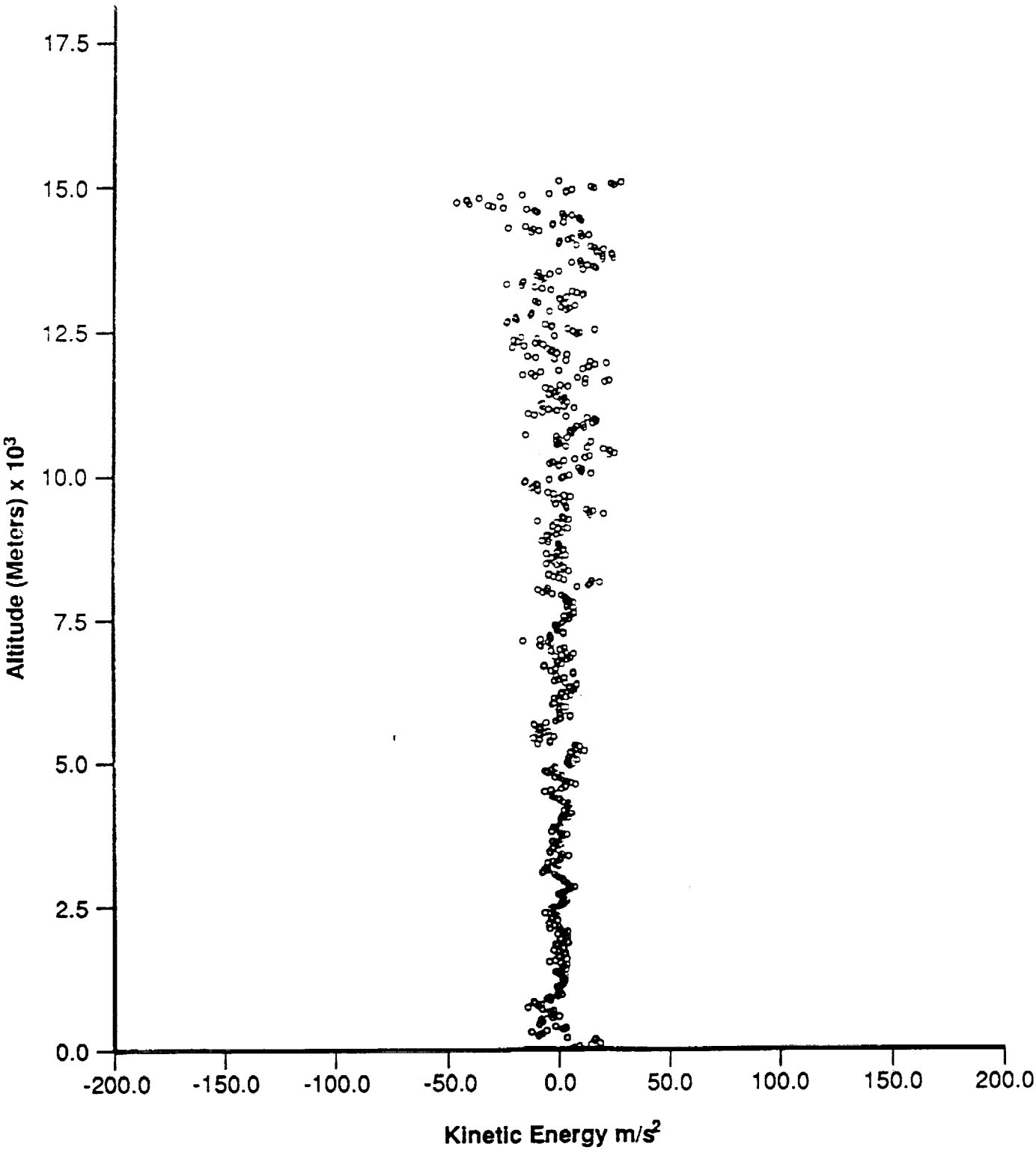

Figure 5g. Kinetic energy versus altitude parameters during STS-51G launch, June 17, 1985 (1133Z) at KSC, Florida.

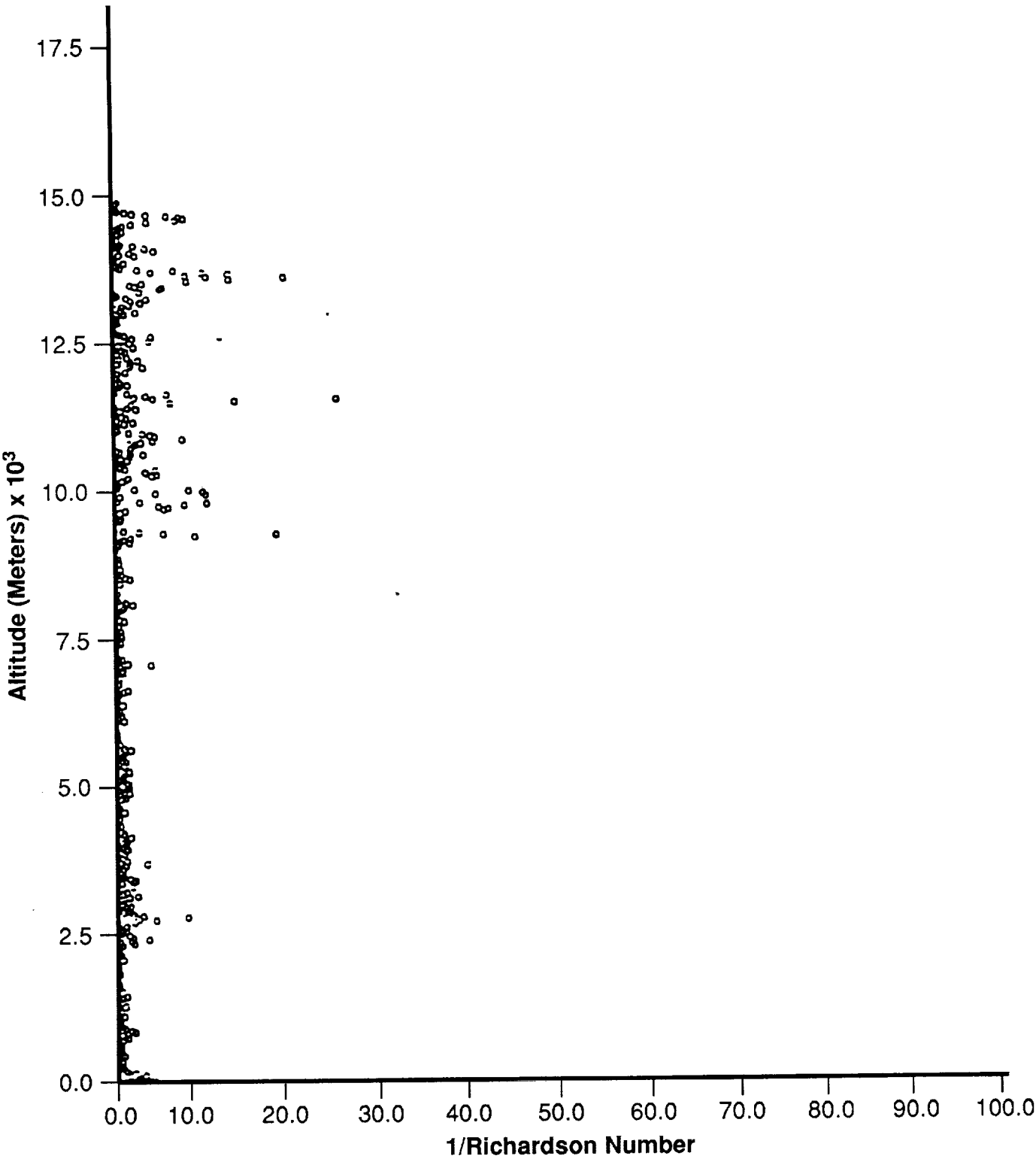

Figure 5h. Richardson number versus altitude parameters during STS-51G launch, June 17, 1985 (1133Z) at KSC, Florida.

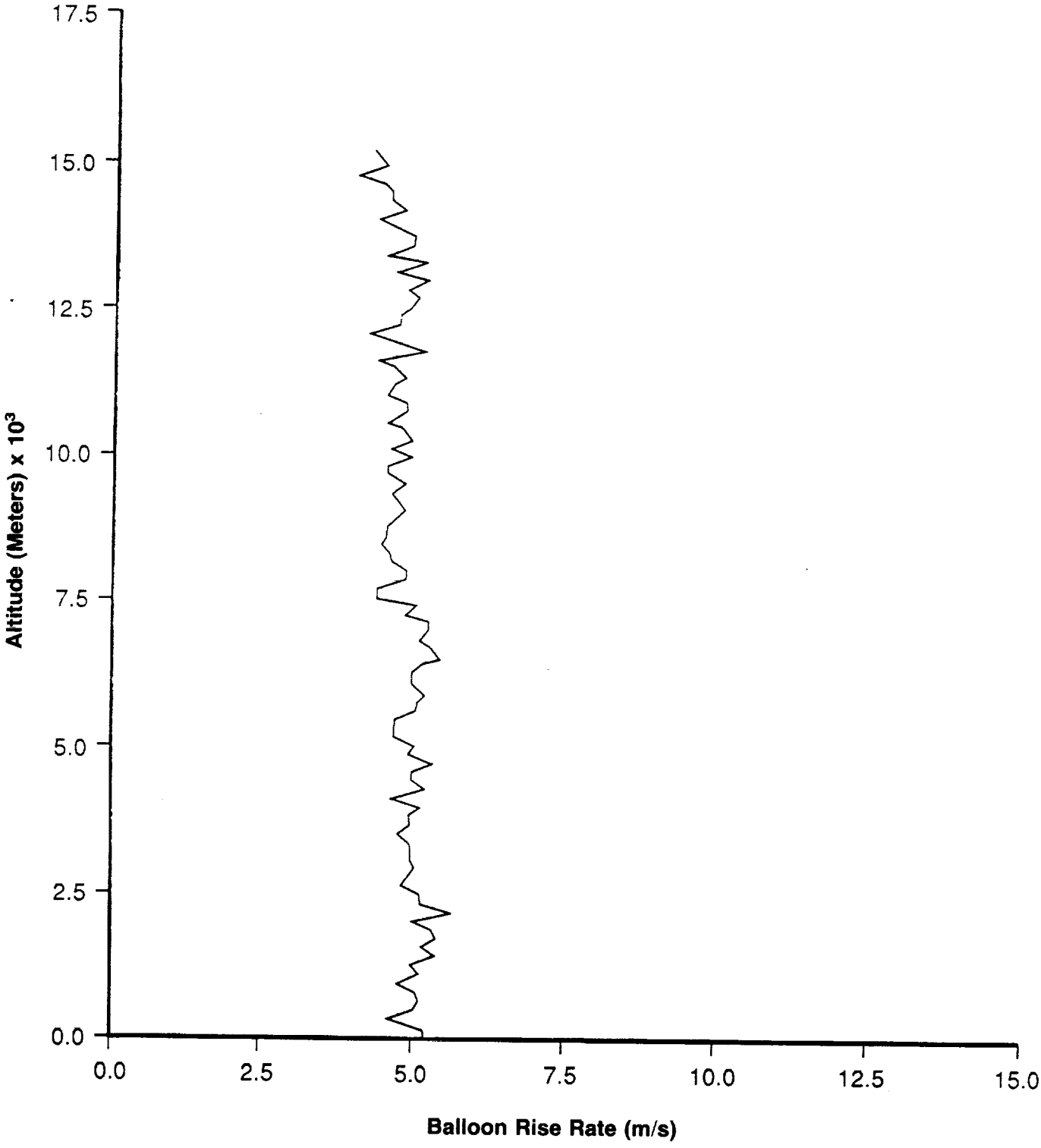

Figure 6a. Rise rate of FPS-16 radar/jimsphere balloon ascent obtained during STS-51F launch, July 29, 1985 (2100Z) at KSC, Florida.

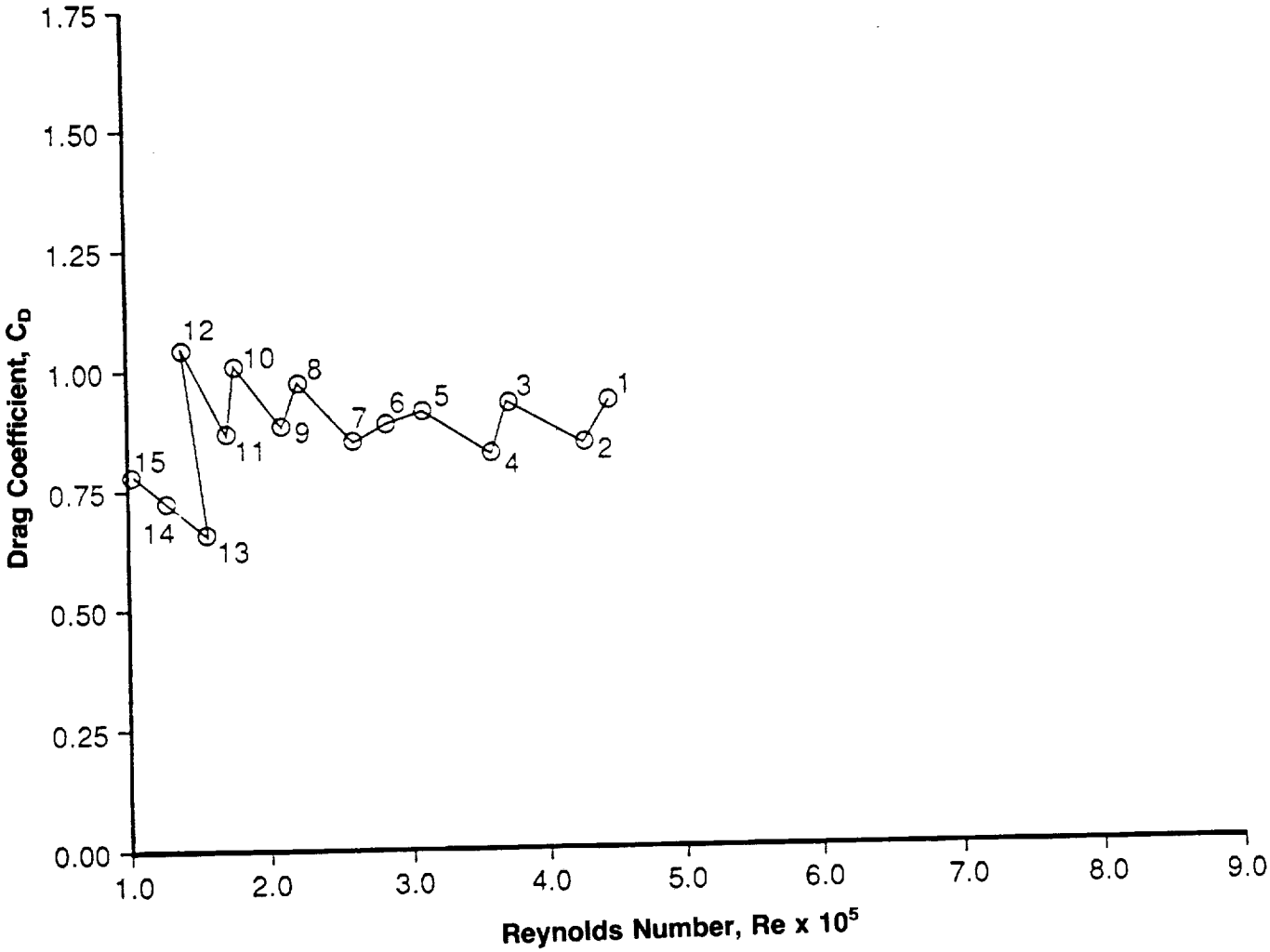

Figure 6b. C_D versus Re parameter obtained from FPS-16 radar/jimsphere balloon ascent during STS-51F launch, July 29, 1985 (2100Z) at KSC, Florida.

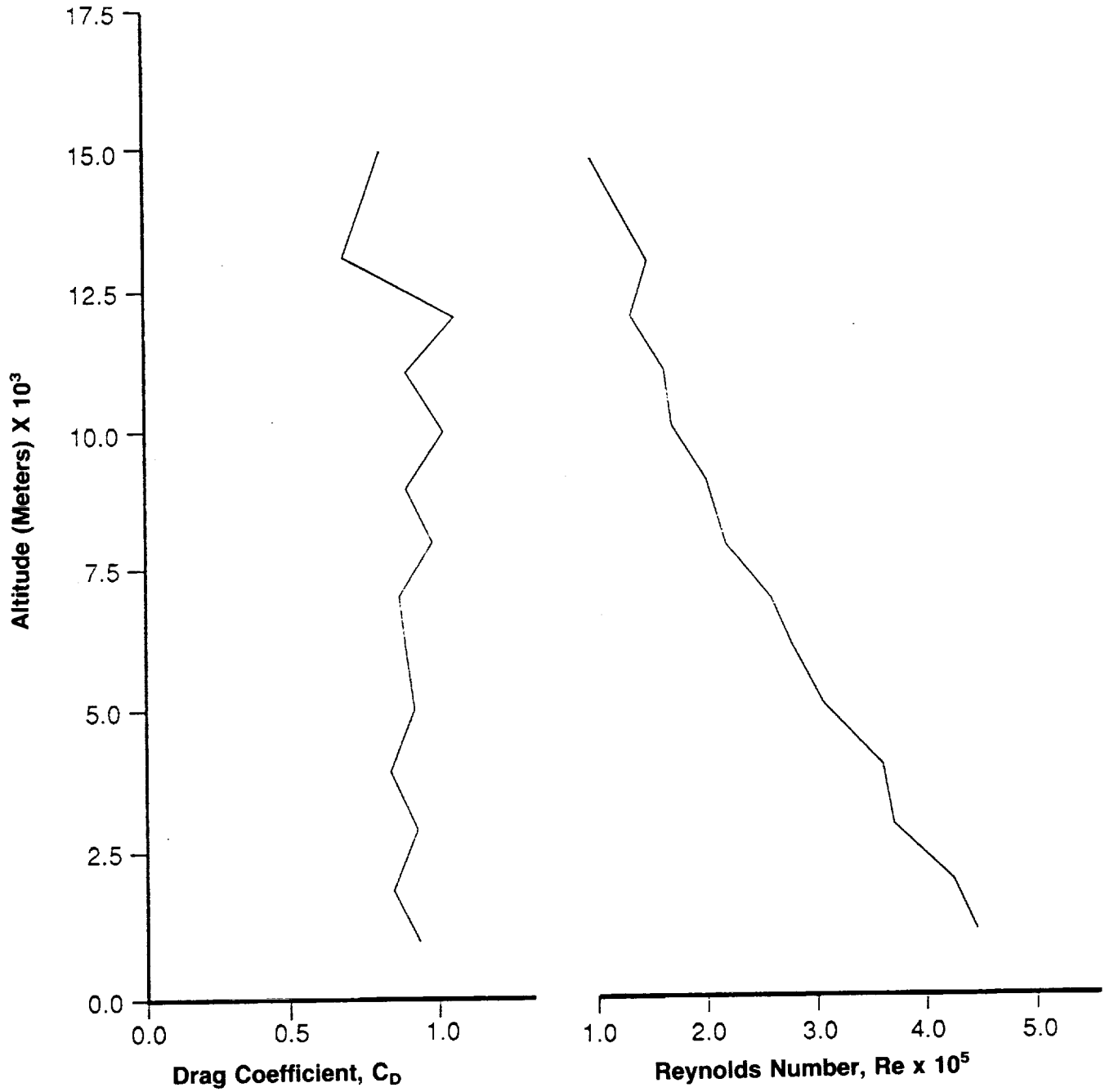

Figure 6c. C_D and *Re* altitude plots obtained from FPS-16 radar/jimsphere balloon ascent during STS-51F launch, July 29, 1985 (2100Z) at KSC, Florida.

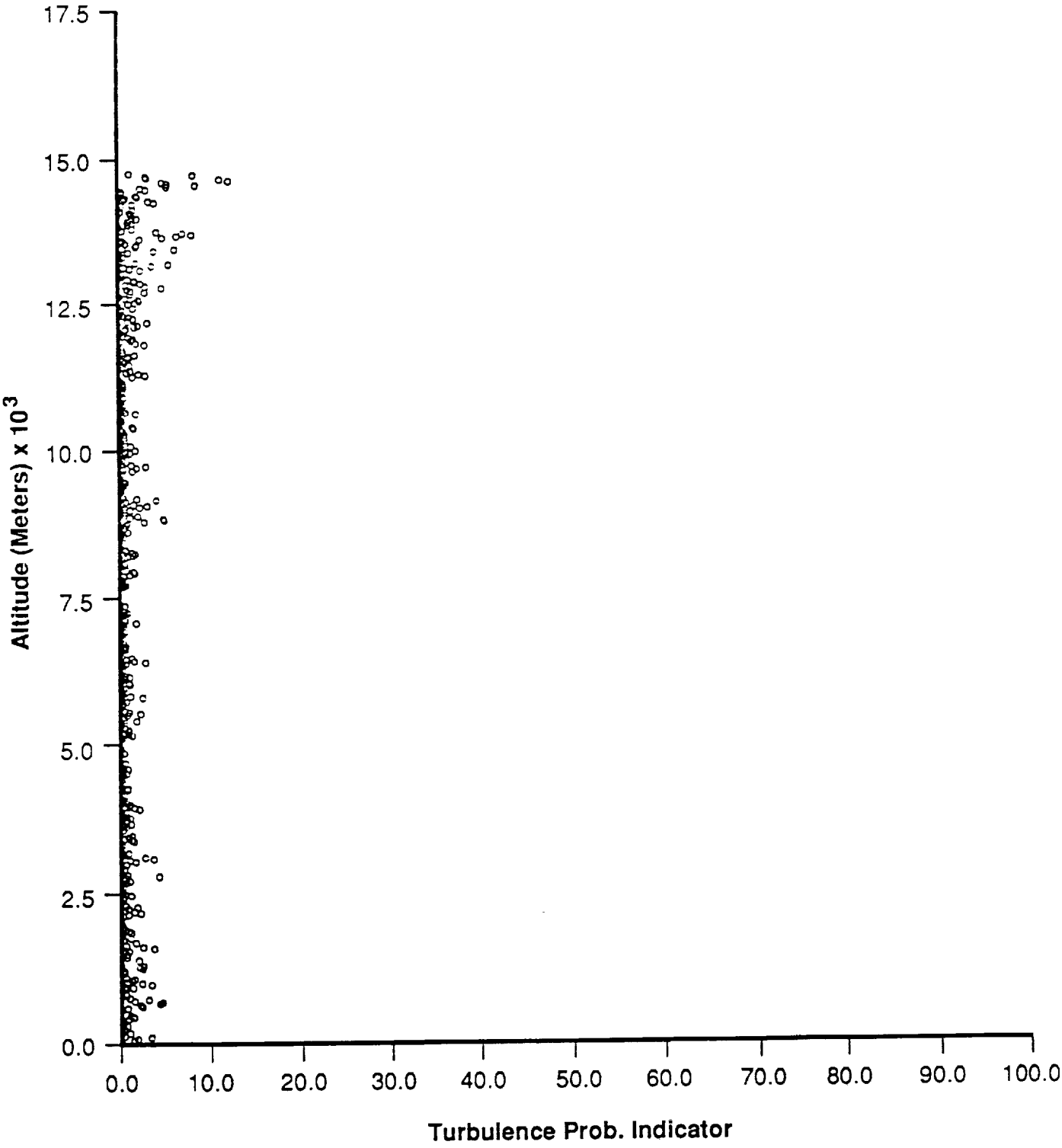

Figure 6d. Turbulence probability indicator obtained during STS-51F launch, July 29, 1985 (2100Z) at KSC, Florida.

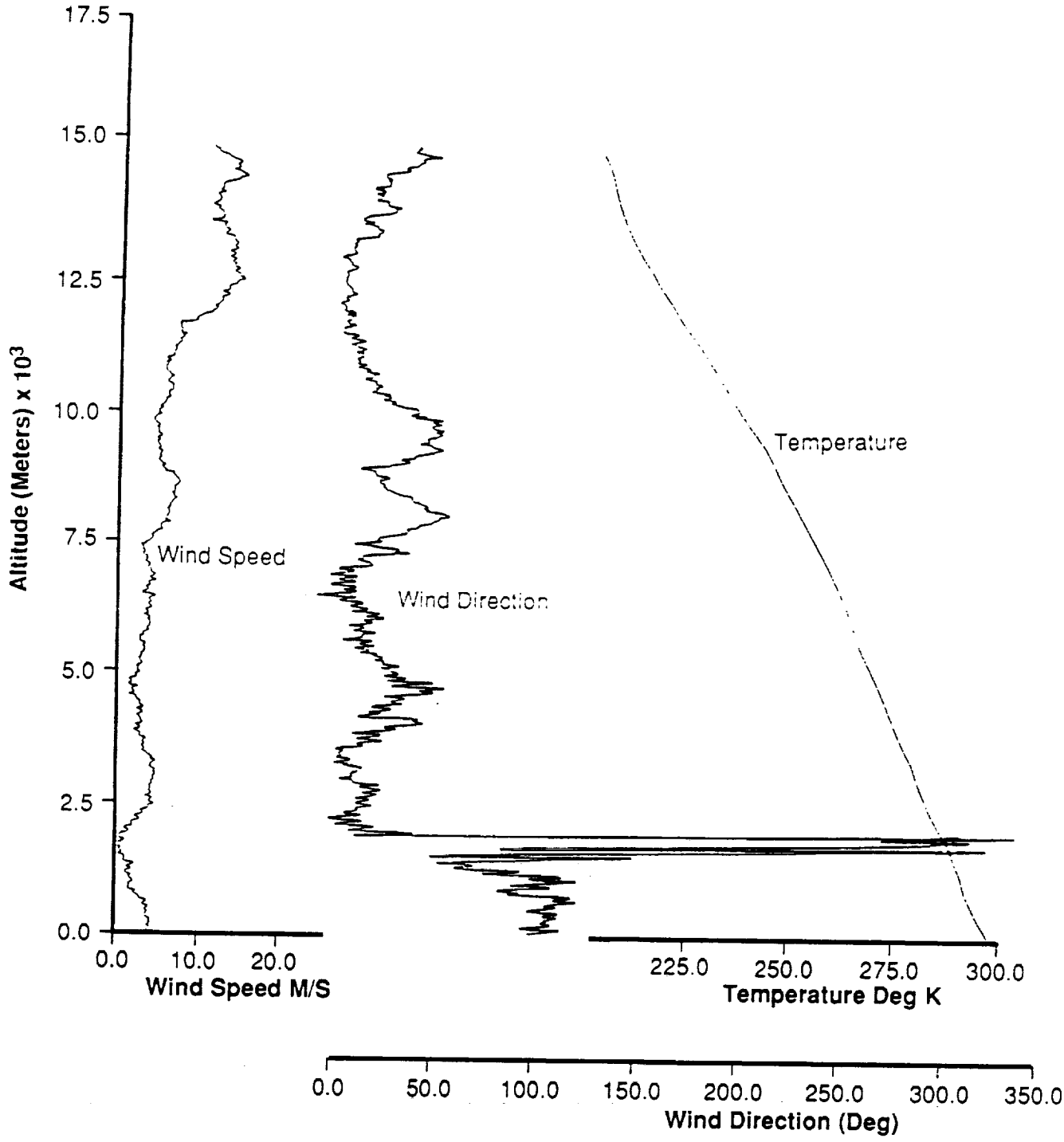

Figure 6e. Wind speed, wind direction, and temperature versus altitude plots measured during STS-51F launch, July 29, 1985 (2100Z) at KSC, Florida.

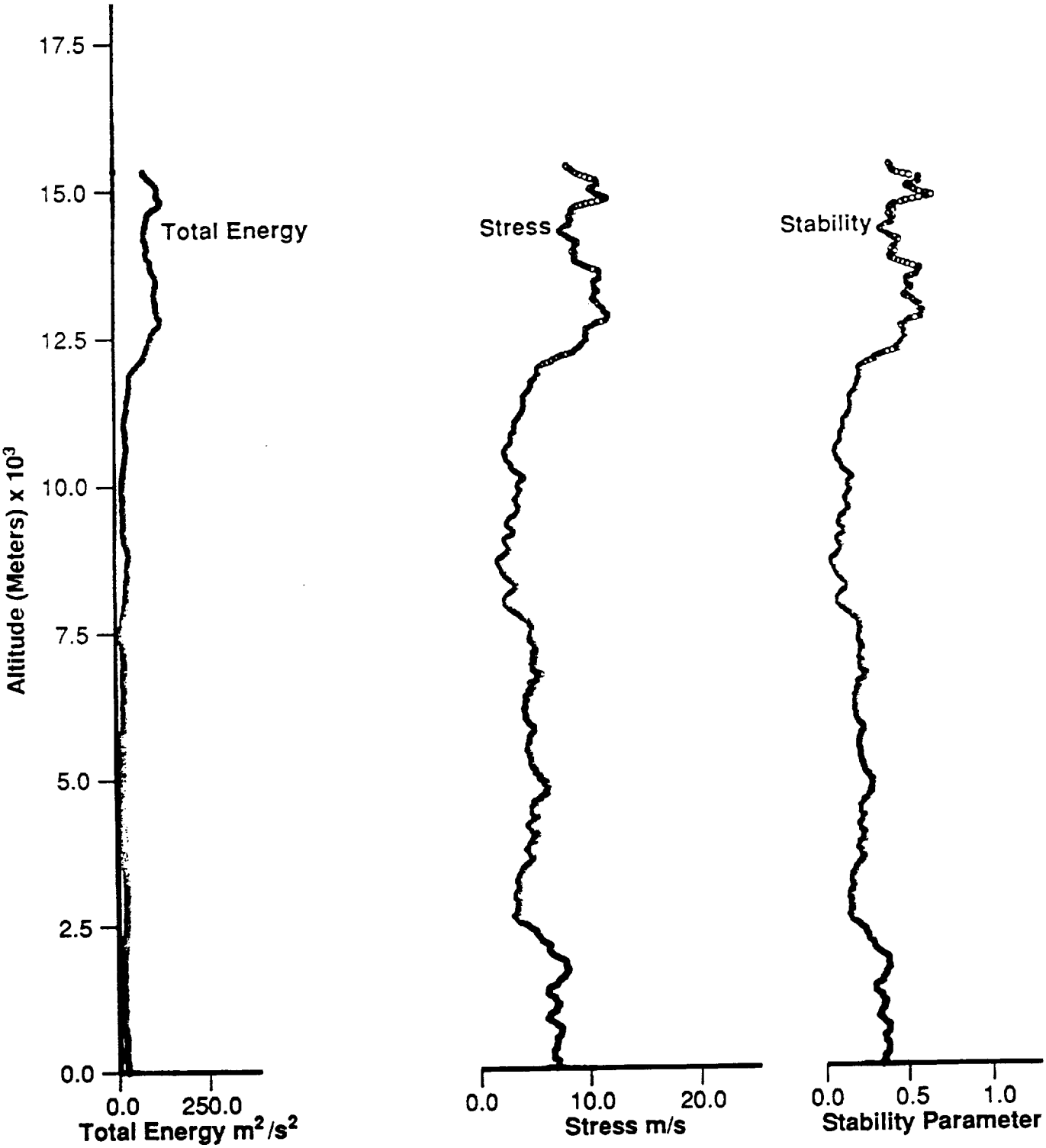

Figure 6f. Total energy, stress, and stability versus altitude parameters for STS-51F launch, July 29, 1985 (2100Z) at KSC, Florida.

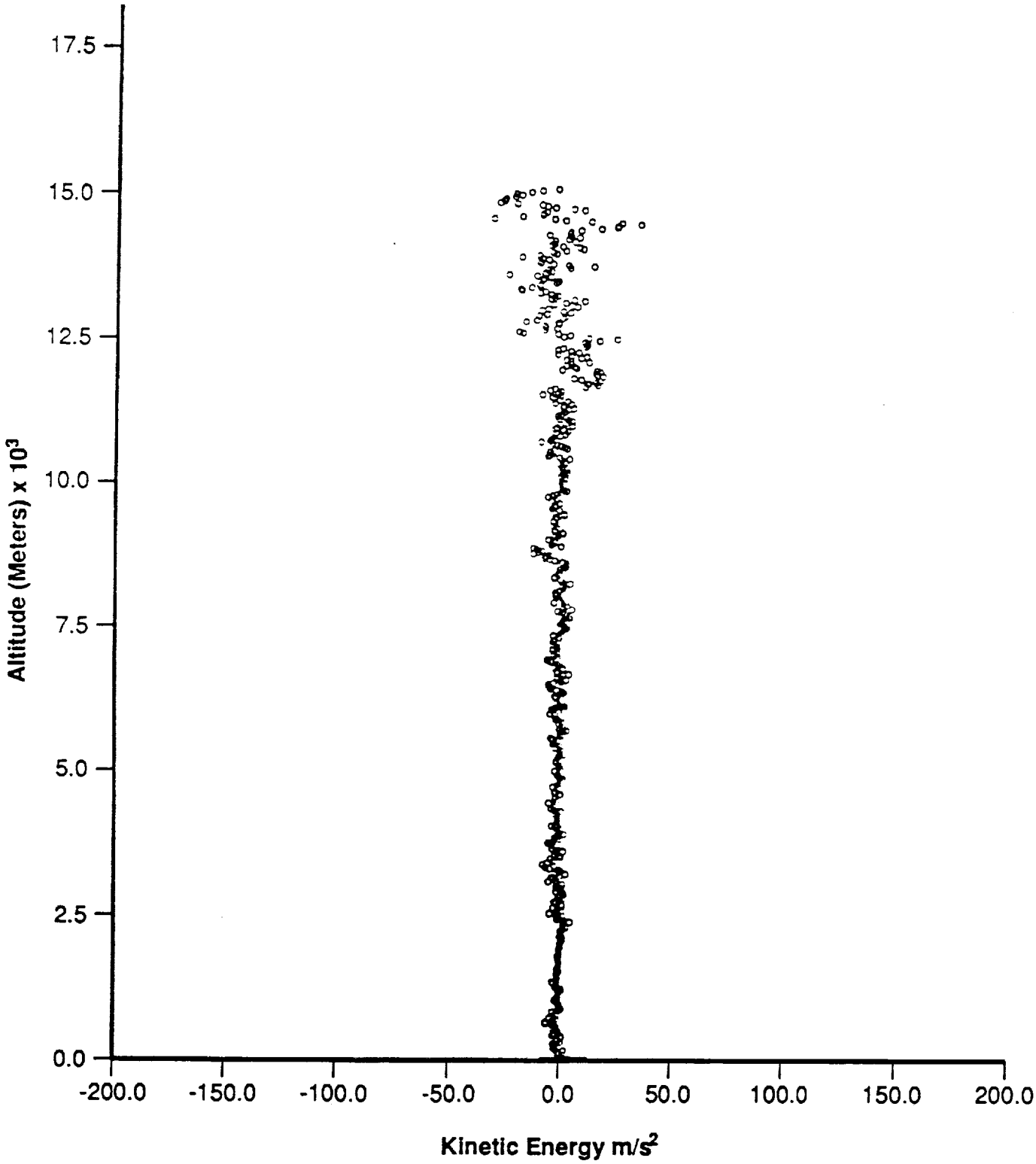

Figure 6g. Kinetic energy versus altitude parameter for STS-51F launch, July 29, 1985 (2100Z) at KSC, Florida.

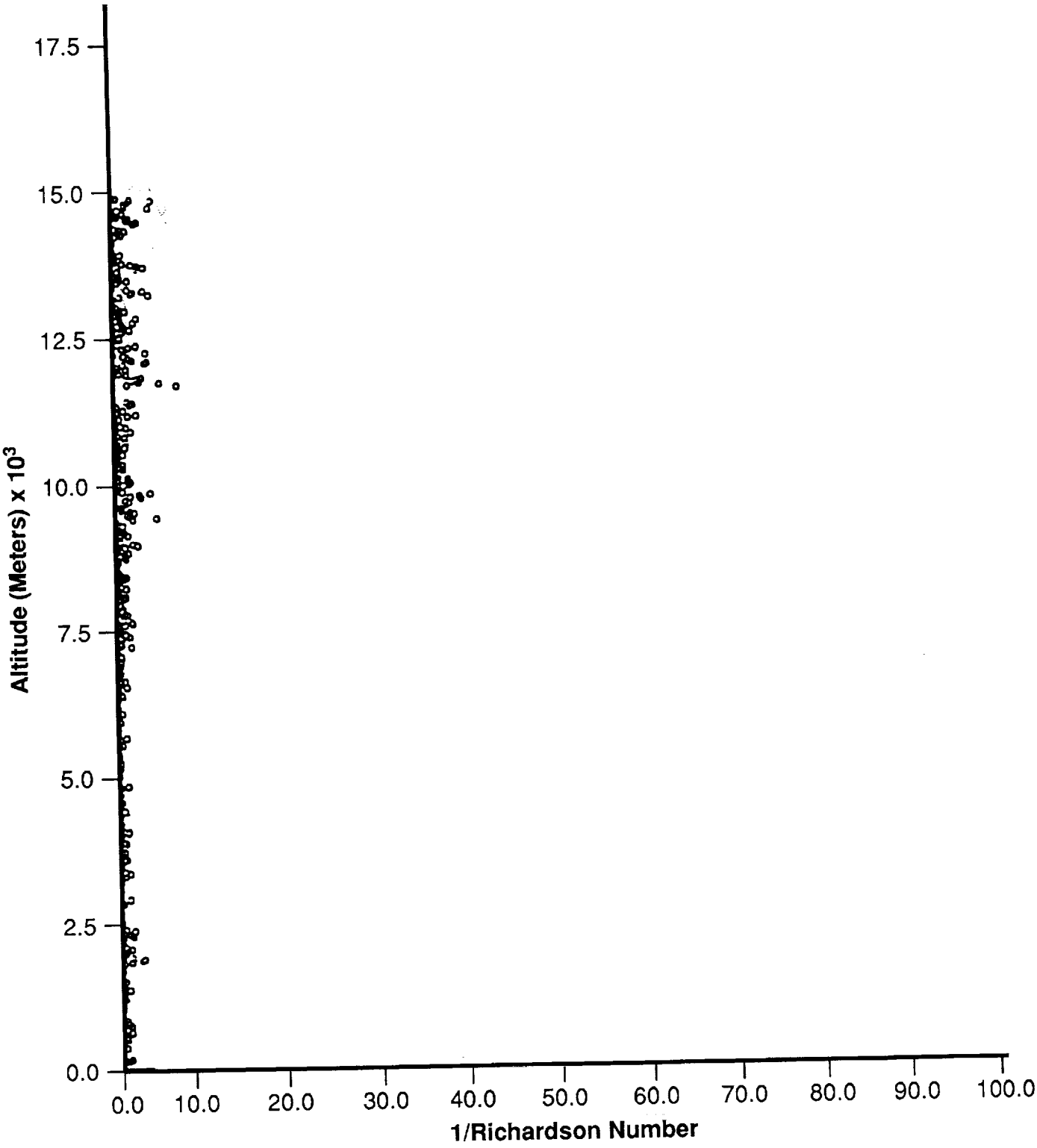

Figure 6h. Richardson number versus altitude parameters for STS-51F launch, July 29, 1985 (2100Z) at KSC, Florida.

REFERENCES

1. Susko, M.: "Analysis of the Bivariate Parameter Wind Differences Between Jimsphere and Windsonde." NASA TM 4014, September 1987.

2. Ehernberger, L.J.: "High Altitude Turbulence for Supersonic Cruise Vehicles." NASA Technical Memorandum 88285, Ames Research Center, Dryden Flight Research Facility, Edwards, California, May 1986.

3. Fairall, C.W., Thomson, D.W., and Syreth, W.J.: "Long Term Studies of the Refractive Index Structure Parameter in the Troposphere and Stratosphere." Penn State Department of Meteorology, University Park, PA, AD-A198313, November 1985 to April 1988.

4. Otten III, L.J., and Rose, W.C.: "Airborne Observations of Tropopause Turbulence." Proceedings of Aerospace Sciences Meeting, 23rd, Reno, NV, 1985.

5. Murtele, M.G.: "Cat Generating Mechanisms." University of California, Los Angeles, CA, April 1987.

6. Huschke, R.E.: "Glossary of Meteorology." American Meteorological Society, Boston, MA, 1959.

7. Dwyer, J.F.: "Factors Affecting the Vertical Motion of a Zero-Pressure, Polyethylene, Free Balloon." AFGL-TR-85-0130, May 1985.

8. Scoggins, J.R.: "Aerodynamics of Spherical Balloon Wind Sensors." Journal of Geophysical Research, vol. 69, April 1967, pp. 591–598.

9. Perevedentsev, Yu. P., and Bogatkin, O.G.: "Atmospheric Turbulence and Its Forecast." Air Force Systems Command, Foreign Technology Division FTD/STINFO, 1984.

10. Endlich, R.M., Singleton, R.C., and Kaufman, J.W.: "Spectral Analysis of Detailed Vertical Wind Speed Profiles." Journal of Atmospheric Science, September 1969, pp. 1030–1041.

11. Fichtl, G.H., Camp, D.W., and Vaughan, W.W.: "Detailed Wind and Temperature Profiles." Clear Air Turbulence and Its Detection, Edited by Yih-He Pao and Arnold Golberg, New York: Plenum Press, 1969.

12. DeMandel, R.E., and Krivo, S.J.: "Radar/Balloon Measurements of Vertical Air Motions Between the Surface and 15 km." Journal of Applied Meteorology, vol. 10, April 1970, pp. 313–319.

13. Kaufman, J.W., and Susko, M.: "Review of Special Detailed Wind and Temperature Profile Measurements." Journal of Geophysical Research, vol. 20, September 1971, pp. 6489–6496.

14. Johnson, D.L., and Vaughan, W.W.: "Sequential High Resolution Wind Profile Measurements." NASA Technical Paper 1354, December 1978.

15. Hill, C.K.: "Analysis of Jimsphere Pairs for Use in Assessing Space Vehicle Ascent Capability." NASA Technical Paper 1354, December 1986.

16. Scoggins, J.R.: "Aerodynamics of Spherical Balloon Wind Sensors." Journal Geophysical Research, vol. 69, February 1964, pp. 591–598.

17. MacCready, P.B., and Jex, H.R.: "Study of Sphere Motion and Balloon Wind Sensors." NASA TM X-53089, February 1964.

18. Vaughan, W.W.: "New Wind Monitoring System Protects Research and Development Launches." Journal of Astronautics and Aeronautics, December 1968, pp. 41–43.

19. Susko, M., and Kaufman, J.W.: "Exhaust Cloud Rise and Growth of Apollo Saturn Engines." Journal of Spacecraft and Rockets, vol. 10, May 1973, pp. 341–345.

20. Susko, M.: "Wind Measurements by Electromagnetic Probes." NASA TM 4066, September 1988.

21. Smith, S.A.: "Cross Spectral Analysis to Determine the Resolutions and Precision of Jimsphere and Windsonde Wind Measurements. Third International Conference on the Aviation Weather System, Anaheim, CA, January 30–February 3, 1989, American Meteorological Society.

22. Susko, M.: "Wind Comparison Analysis of Pibal Versus Anemometer." NASA TMX-53663, October 1967.

23. Mikkelsen, T., Hansen, A., Eckman, R.M., and Thykier-Nielsen, S.: "Project WIND, Phase IV, Dispersion Study: Aerial Smoke Plume Observations and Surface Layer Turbulence Measurements, Part 1." Rise-M-2718, Roskilde, Denmark, January 1989.

24. Endlich, R.M.: "The Probable Final Cause of the Challenger Accident—Clear Air Turbulence in the Jet Stream." AERA 89-2, Los Altos, CA, January 1989.

NASA
National Aeronautics and Space Administration

Report Documentation Page

1. Report No.	2. Government Accession No.	3. Recipient's Catalog No.
NASA TM-4289		

4. Title and Subtitle	5. Report Date
Atmospheric Turbulence Review of Space Shuttle Launches	May 1991
	6. Performing Organization Code: ES44

7. Author(s)	8. Performing Organization Report No.
Michael Susko	
	10. Work Unit No.: M-660

9. Performing Organization Name and Address	11. Contract or Grant No.
George C. Marshall Space Flight Center Marshall Space Flight Center, Alabama 35812	
	13. Type of Report and Period Covered: Technical Memorandum

12. Sponsoring Agency Name and Address	14. Sponsoring Agency Code
National Aeronautics and Space Administration Washington, DC 20546	

15. Supplementary Notes

Prepared by Space Sciences Laboratory, Science and Engineering Directorate.

16. Abstract

The primary objective of this paper is to report on the research and analysis on identifying turbulent regions from the surface to 16 km for space shuttle launches. This research has demonstrated that the results from the FPS-16 radar/jimsphere balloon system in measuring winds can indeed indicate the presence or conditions ripe for turbulence in the troposphere and lower stratosphere. It is further demonstrated that atmospheric data obtained during the shuttle launches by the rawinsonde in conjunction with the jimsphere provides the necessary meteorological data to compute aerodynamic parameters to identify turbulence, such as Reynolds number, drag coefficient, turbulent stresses, total energy, stability parameter, vertical gradient of kinetic energy, Richardson number, and the turbulence probability index. There is no magic fool-proof criteria in atmospheric turbulent probability of occurrence. However, enhanced temperature lapse rates and inversion rates, strong vector wind shears, and large changes in wind direction identify the occurrence of turbulence at the tropopause. When any two of the above conditions occur simultaneously, a significant probability of turbulence can occur as shown in the paper.

17. Key Words (Suggested by Author(s))	18. Distribution Statement
Tropopause, Inversion Layer, Stratosphere, Turbulence, Maximum Dynamic Pressure	Unclassified – Unlimited Subject Category: 18

19. Security Classif. (of this report)	20. Security Classif. (of this page)	21. No. of pages	22. Price
Unclassified	Unclassified	68	A04

NASA FORM 1626 OCT 86

For sale by the National Technical Information Service, Springfield, VA 22161-2171

NASA-Langley, 1991